

UC Riverside

UC Riverside Previously Published Works

Title

Evolutionary systems biology reveals patterns of rice adaptation to drought-prone agro-ecosystems.

Permalink

<https://escholarship.org/uc/item/99m5k2b0>

Journal

The Plant Cell, 34(2)

ISSN

1040-4651

Authors

Groen, Simon C
Joly-Lopez, Zoé
Platts, Adrian E
[et al.](#)

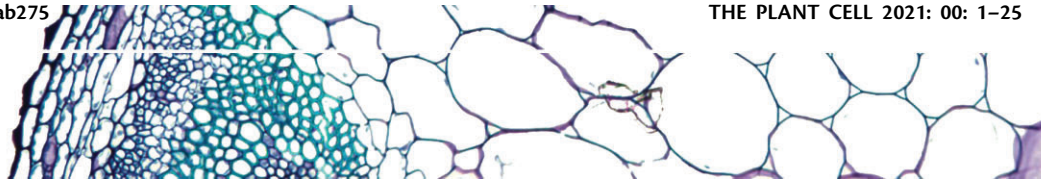
Publication Date

2022-02-03







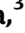


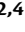


DOI

10.1093/plcell/koab275

Peer reviewed



Evolutionary systems biology reveals patterns of rice adaptation to drought-prone agro-ecosystems

Simon C. Groen ^{1,2,*}, Zoé Joly-Lopez ^{2,†}, Adrian E. Platts ^{2,‡}, Mignon Natividad ³,
Zoë Fresquez ², William M. Mauck III ⁴, Marinell R. Quintana ³, Carlo Leo U. Cabral ³,
Rolando O. Torres ³, Rahul Satija ^{2,4}, Michael D. Purugganan ^{2,5,*} and Amelia Henry ^{3,*}

- 1 Institute of Integrative Genome Biology and Department of Nematology, University of California at Riverside, Riverside, California, USA
- 2 Center for Genomics and Systems Biology, Department of Biology, New York University, New York, USA
- 3 International Rice Research Institute, Los Baños, Laguna, Philippines, USA
- 4 New York Genome Center, New York, USA
- 5 Center for Genomics and Systems Biology, NYU Abu Dhabi Research Institute, New York University Abu Dhabi, Saadiyat Island, Abu Dhabi, UAE

*Author for correspondence: simon.groen@ucr.edu (S.C.G.), mp132@nyu.edu (M.D.P.), a.henry@irri.org (A.H.).

[†]Present address: Département de Chimie, Université du Québec à Montréal, Montréal, Québec, Canada.

[‡]Present address: Department of Plant Biology, Michigan State University, East Lansing, Michigan, USA.

[§]Senior authors.

Conceived and directed the project: S.C.G., M.D.P., and A.H.; Designed and coordinated field experiments: A.H., R.O.T., and S.C.G.; Performed field experiments: M.N., C.L.U.C., R.O.T., Z.J.-L., and S.C.G.; Processed samples and extracted RNA for sequencing: Z.F., M.N., Z.J.-L., and S.C.G.; Made RNA-seq libraries: W.M.M.; Designed and ran bioinformatics workflow for RNA-seq: A.E.P., and R.S.; Conducted genetic marker-based analyses: Z.J.-L., A.E.P., and S.C.G.; Processed fitness, functional trait and gene expression data, and performed statistical analyses: M.N., M.R.Q., A.H., and S.C.G.; Wrote the manuscript: S.C.G., M.D.P., and A.H.

The authors responsible for distribution of materials integral to the findings presented in this article in accordance with the policy described in the Instructions for Authors (<https://academic.oup.com/plcell>) are: Simon C. Groen (simon.groen@ucr.edu), Michael D. Purugganan (mp132@nyu.edu), and Amelia Henry (a.henry@irri.org).

Abstract

Rice (*Oryza sativa*) was domesticated around 10,000 years ago and has developed into a staple for half of humanity. The crop evolved and is currently grown in stably wet and intermittently dry agro-ecosystems, but patterns of adaptation to differences in water availability remain poorly understood. While previous field studies have evaluated plant developmental adaptations to water deficit, adaptive variation in functional and hydraulic components, particularly in relation to gene expression, has received less attention. Here, we take an evolutionary systems biology approach to characterize adaptive drought resistance traits across roots and shoots. We find that rice harbors heritable variation in molecular, physiological, and morphological traits that is linked to higher fitness under drought. We identify modules of co-expressed genes that are associated with adaptive drought avoidance and tolerance mechanisms. These expression modules showed evidence of polygenic adaptation in rice subgroups harboring accessions that evolved in drought-prone agro-ecosystems. Fitness-linked expression patterns allowed us to identify the drought-adaptive nature of optimizing photosynthesis and interactions with arbuscular mycorrhizal fungi. Taken together, our study provides an unprecedented, integrative view of rice adaptation to water-limited field conditions.

IN A NUTSHELL

Background: Rice (*Oryza sativa*) was domesticated around 10,000 years ago and has since become a staple for over half the global human population. Over this time, rice has been grown in various agro-ecosystems that differ in their patterns of water availability, one of the most important for smallholder farmers being the rainfed lowland system. How rice has adapted to frequent drought in this system remains poorly understood. While previous field studies discovered that optimization of flowering time and morphological traits helps plants adapt to drought stress, variation in hydraulic components (affecting water movement within the plant) and molecular traits such as gene expression has received less attention, particularly in roots.

Question: We wanted to find out which molecular and physiological traits in roots and shoots allow rice varieties from drought-prone agro-ecosystems to maximize fitness (yield) under drought.

Findings: We set up a two-year field study in which we planted 20+ diverse rice varieties in wet and dry lowland conditions in the Philippines and found that stable genetic variation in molecular and hydraulic traits is correlated with higher rice fitness under drought. In both roots and shoots we discovered modules (groups) of co-expressed genes that are linked with these traits. These expression modules revealed not only that a multitude of genes is involved in adaptation to water limitation among rice varieties that evolved in drought-prone agro-ecosystems, but also that intensifying root interactions with arbuscular mycorrhizal fungi could benefit rice when faced with drought.

Next steps: We will follow up on our findings by functionally characterizing several of the genes that appear to be under selection and linked to rice fitness under drought, with the aim of establishing how expression of these genes in roots and shoots underlies adaptive variation in hydraulic traits. We will also explore how root interactions with other soil organisms such as plant-parasitic nematodes might differ between wet and dry conditions. Ultimately, it might be possible to use the gene modules we identified as guides in breeding programs for resilient rice.

Introduction

The chemical equation for photosynthesis, $6\text{CO}_2 + 6\text{H}_2\text{O} + \text{light energy} > \text{C}_6\text{H}_{12}\text{O}_6 + 6\text{O}_2$, illustrates that plants cannot maintain high levels of carbon fixation when water availability is limited (Calvin, 1956). In response to environments with restricted or variable water availability, plants have evolved intricate mechanisms that continue to fix resources and maximize survival and seed production (fitness) under drought: (1) drought escape, (2) drought avoidance, and (3) drought tolerance (Levitt, 1980). Escape can be realized through constitutive or drought-induced early flowering. The latter is a form of phenotypic plasticity in which a plant expresses different trait values across varying environments (Nicotra et al., 2010). Mechanisms of flowering time regulation have been characterized relatively well (Shrestha et al., 2014). We have recently identified genes, including one encoding the transcription factor (TF) MCM AGAMOUS DEFICIENS SRF18 (OsMADS18, Os07g605200), that contribute to drought escape in rice by studying patterns of covariation between shoot gene expression, flowering time, and fitness (Groen et al., 2020).

However, much less progress has been made in characterizing adaptive variation in drought avoidance and tolerance, because these are complex mechanisms that involve tightly regulated processes at the biochemical, physiological, and whole-plant levels. Like drought escape, drought avoidance and tolerance can be realized through baseline (constitutive) trait values, through drought-induced changes in trait values (plasticity), or a combination thereof (Nicotra et al., 2010; Sandhu et al., 2016). Drought avoidance may on the one

hand involve enhanced water uptake via rapid plastic responses in root hydraulics and/or architecture—a “water-spending” strategy—and on the other hand involve reduced water loss through changes in leaf area and orientation as well as stomatal conductance—a “water-saving” strategy (Tardieu and Simonneau, 1998). Measurements of stomatal conductance, in conjunction with photosynthetic carbon gain, can be used for determining water use efficiency (WUE; Levitt, 1980). Drought tolerance involves the maintenance of cell turgor through osmotic adjustment or cell wall elasticity, the maintenance of antioxidant capacity, and desiccation tolerance (Levitt, 1980). Signaling via abscisic acid (ABA), auxin, and other phytohormones, plays a vital role in regulating these three drought resistance strategies (Todaka et al., 2015; Gupta et al., 2020).

Rice is a staple food for >50% of the global population (Wing et al., 2018). Domesticated rice can be divided into the *circum*-aus, indica, japonica, and *circum*-basmati subgroups (Huang et al., 2012a; Wang et al., 2018). While the traditional varieties or landraces that make up the temperate japonica, sub-tropical japonica, and *circum*-basmati subgroups have predominantly evolved in irrigated agro-ecosystems, landraces in the *circum*-aus, indica, and tropical japonica subgroups have also adapted multiple times independently to drought-prone rainfed agro-ecosystems (Gutaker et al., 2020). Finding out the drought resistance strategies that have been selected for in rice, how these strategies are integrated at the whole-plant level, and which regions of the genome regulate them in field settings could inform ongoing efforts to breed and engineer resilient new varieties (Wing et al., 2018).

Traditional forward and reverse genetic mapping approaches, at times combined with RNA sequencing (RNA-seq), have been successful for characterizing the genetic architecture of shoot and root drought resistance traits in carefully controlled plant growth settings, and some candidate genes have been functionally verified (Gupta et al., 2020). Yet, it is not clear how genetic variation in drought resistance strategies relates to the performance of plants at the whole-plant level and how they function in reducing drought damage to fitness-related traits. More insight into how molecular and physiological traits act in concert with morphological traits, and how root and shoot responses to stress are integrated in field environments, is necessary (Des Marais et al., 2012; Groen, 2016; Henry et al., 2016; Gupta et al., 2020). The latter point is of particular importance in light of the growing realization that there is a lab–field gap (Groen and Purugganan, 2016; Poorter et al., 2016; Zaidem et al., 2019): molecular measurements are typically done in controlled laboratory environments, but plant responses to stress in these circumstances are not fully reflective of how plants react to fluctuating field conditions (Nagano et al., 2012; Richards et al., 2012; Plessis et al., 2015; Wilkins et al., 2016; Swift et al., 2019; Groen et al., 2020; Kawakatsu et al., 2021). Sources of these differences include biotic interactions of plant roots with soil-inhabiting animals and microorganisms such as plant-parasitic nematodes, herbivorous insects, rhizobacteria, arbuscular mycorrhizal fungi (AMF), and endophytic fungi (Groen and Purugganan, 2016; Poorter et al., 2016; Zaidem et al., 2019; de Vries et al., 2020). While these interactions are often kept to a minimum in laboratory environments, they can have decisive modulating effects on how drought affects plants (Mbodj et al., 2018; de Vries et al., 2020).

Here, we take an evolutionary systems biology approach, where we characterize morphological and physiological shoot and root trait variation in a rice diversity panel growing in wet or water-limited field conditions and try to better understand how this variation is tied to fitness. We then study the molecular basis of these traits by identifying gene co-expression modules linked to adaptive trait variation, and test if these modules show hallmarks of longer term selection within domesticated rice. Finally, we validate biological processes enriched in modules relevant to fitness by measuring related functional traits and assess their correlations with fitness in a subsequent crop season.

Results

Rice shows genetic variation for drought escape and avoidance traits

We assembled a core panel of 22 diverse rice accessions from all main subgroups (Supplemental Figure S1 and Supplemental Data Set S1; Huang et al., 2012a; Wang et al., 2018). Most were landraces that have evolved in stably wet irrigated lowland agro-ecosystems, as well as more drought-prone deepwater, rainfed lowland and upland systems, which might be excellent sources of drought resistance-

related genetic variants (Torres et al., 2013; Kumar et al., 2014; Groen et al., 2020; Gutaker et al., 2020). Based on our previous observations (Groen et al., 2020), we selected accessions for our core panel to have narrower flowering time and leaf size windows around the population means than our larger diversity panel with the aim of preventing the strong link between drought escape and plant fitness from overshadowing signals for drought avoidance or tolerance (Supplemental Figure S1).

We then planted identical sister populations (four biological replicate plots per accession) in two lowland fields in the Philippines in the 2017 dry season: a continuously wet field (flooded paddy), and a field where plants were exposed to intermittent drought in the vegetative and reproductive stages (Figure 1; Supplemental Figure S2 and Supplemental Data Sets S2 and S3). One accession, Hsinchu 51, displayed dwarfed growth and yellowing, even when not water-limited, and was excluded from all analyses. We studied drought escape by measuring flowering time and assessed drought avoidance through measuring a series of morphological and physiological root and shoot traits (Table 1). For root traits, this involved quantifying the xylem sap exudation rate (Henry et al., 2012), and measuring root density through reconstruction of crown root architecture with the digital imaging of root traits (DIRT) platform (Bucksch et al., 2014; Das et al., 2015). We also studied drought tolerance by analyzing the biochemical traits of leaf and root osmotic potential (Ψ_{leaf} , Ψ_{root}), and the ratio between them ($\Psi_{\text{leaf}}/\text{root}$). As proxies for plant fitness, we measured the yield of straw and filled grains produced per square meter (by dry weight). We also included panicle length and the harvest index (ratio of filled grain dry weight to total shoot dry weight).

All drought escape and avoidance traits, except early shoot dry weight, generally showed significant genetic variation (measured as broad-sense heritability, H^2), whereas the drought tolerance traits did not (Tables 1 and 2; Supplemental Data Set S2). These results show that phenological drought escape traits as well as morphological and physiological drought avoidance traits could be used in breeding if they improve drought resistance. Drought tolerance traits did not show significant genetic variation in our study, presumably owing to higher levels of micro-environmental plasticity in these noisily fluctuating biochemical traits (Henry et al., 2016). However, they could still contribute to drought resistance.

Several drought avoidance and tolerance traits are associated with fitness

Next, we tested which traits were genetically associated with measures of plant fitness, either in terms of their baseline trait values in the dry environment and/or in terms of their plasticity. Plasticity was measured as the simplified relative distance plasticity index (RDPI_s), which represents the absolute difference of mean genotypic trait values across environments divided by the mean genotypic trait value in the wet

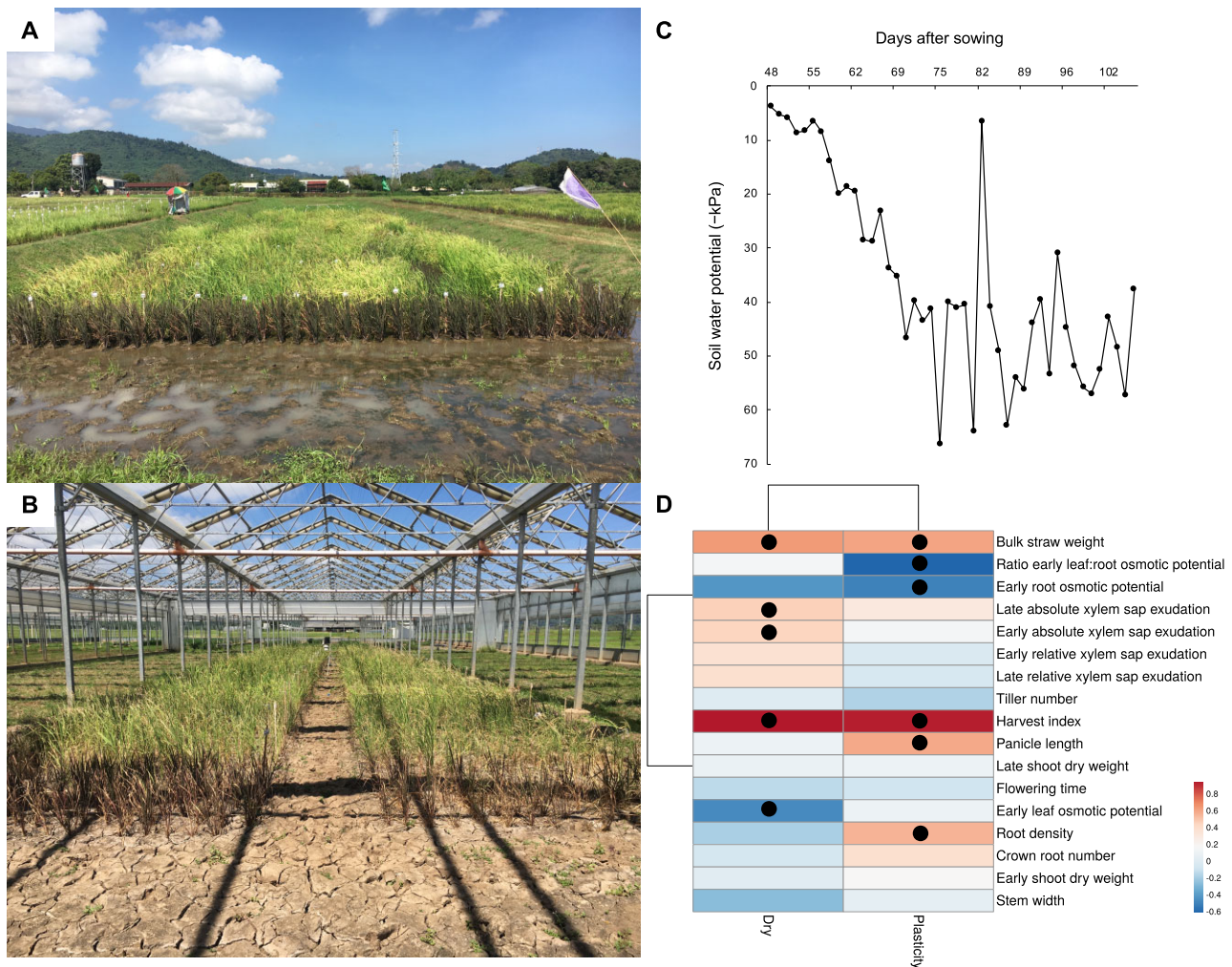


Figure 1 Root physiological parameters are linked to fitness under drought. A, A panel of 22 diverse rice accessions with representatives of all major subgroups (planted with four replicates in a randomized complete block design) was monitored for a series of morphological, physiological and molecular traits. B, The same panel was phenotyped in a rain-out shelter under simulated drought with plots laid out in a design that was identical to the one in the continuously wet paddy. C, Fluctuations of the deficit in soil water potential over the 2017 dry season. D, The heatmap shows Pearson product-moment correlation coefficients between baseline trait values and trait plasticity values of drought resistance traits on the one hand and the fitness component bulk filled grain weight on the other ($n = 21$). Baseline trait values in the dry field were assessed for correlations with fitness in the dry field. Plasticity values were estimated by calculating the RDPI_s ("Materials and Methods") for each trait in each genotype between the wet and dry fields and assessed for correlations with combined fitness values for both fields. Dots indicate significant correlations ($P < 0.05$).

environment (Valladares et al., 2006; Sandhu et al., 2016). Both fitness component traits were significantly positively correlated with one another, as well as with harvest index, in both wet and dry conditions (Pearson's $r \geq 0.6199$, $P \leq 0.0024$). This was also the case for the plasticity of fitness component traits (Pearson's $r \geq 0.5949$, $P \leq 0.0044$). Thus, we focused our analyses for the 2017 dry season on filled grain yield as our fitness proxy (Supplemental Data Set S4).

As expected for this panel chosen to have a narrow flowering time window, drought escape was not significantly linked to fitness: not as flowering time in the dry field (Pearson's $r = -0.1303$, $P = 0.5733$), and neither as flowering time plasticity (Pearson's $r = -0.0955$, $P = 0.6804$;

Figure 1D). On the other hand, several physiological and morphological traits were indeed linked to fitness under drought. We observed positive fitness correlations for plasticity in panicle length as well as for the drought avoidance traits absolute xylem sap exudation (early and late) and plasticity in root density (Pearson's $r \geq 0.4362$, $P \leq 0.0481$). In particular, high-fitness accessions displayed increased crown root density under drought, despite having lower absolute crown root numbers in these conditions (Table 2). The drought tolerance traits early Ψ_{leaf} and plasticity in early Ψ_{root} and $\Psi_{\text{leaf/root}}$ showed negative correlations with fitness (Pearson's r less than or equal to -0.455 , $P \leq 0.0382$; Figure 1D).

Table 1 Summary statistics for drought resistance and fitness component traits in the rice core panel across dry and wet environments

| Type | Trait | Wet environment | | | | | Dry environment | | | | | | |
|------|----------------------|-----------------|---------|--------|---------|--------|-----------------|----|---------|--------|---------|--------|---------|
| | | N | Mean | SEM | StDev | Min | Max | N | Mean | SEM | StDev | Min | Max |
| DA | Early SDW | 83 | 0.653 | 0.043 | 0.390 | 0.03 | 1.55 | 84 | 1.408 | 0.064 | 0.587 | 0.33 | 3.14 |
| DA | Late SDW | 84 | 5.213 | 0.325 | 2.980 | 0.94 | 13.72 | 84 | 4.521 | 0.286 | 2.617 | 1.07 | 15.75 |
| DA | Early rXSE | 83 | 1.539 | 0.058 | 0.530 | 0.135 | 3.05 | 84 | 1.111 | 0.044 | 0.408 | 0.360 | 2.229 |
| DA | Late rXSE | 83 | 1.485 | 0.074 | 0.677 | 0.465 | 3.897 | 83 | 0.218 | 0.013 | 0.122 | 0.042 | 0.668 |
| DA | Early aXSE | 83 | 0.931 | 0.057 | 0.517 | 0.014 | 1.988 | 84 | 1.457 | 0.088 | 0.803 | 0.347 | 7 |
| DA | Late aXSE | 83 | 6.563 | 0.324 | 2.953 | 2.2 | 15.27 | 84 | 0.968 | 0.086 | 0.790 | 0.25 | 3.7 |
| DA | Stem width | 84 | 0.253 | 0.006 | 0.053 | 0.163 | 0.390 | 84 | 0.199 | 0.005 | 0.049 | 0.099 | 0.334 |
| DA | Tiller nr | 84 | 10.060 | 0.464 | 4.255 | 3 | 31 | 84 | 5.845 | 0.306 | 2.801 | 1 | 14 |
| DA | Crown root nr | 84 | 323.083 | 12.080 | 110.713 | 62 | 573 | 84 | 71.857 | 3.294 | 30.189 | 16 | 151 |
| DA | Crown root density | 84 | 2.413 | 0.156 | 1.427 | 0.776 | 9.178 | 84 | 5.843 | 0.391 | 3.587 | 0.882 | 19.890 |
| DT | Early LOP | 82 | 554.341 | 6.568 | 59.477 | 411 | 678 | 84 | 537.833 | 6.251 | 57.294 | 410 | 720 |
| DT | Early ROP | 84 | 89.964 | 3.090 | 28.322 | 39 | 180 | 84 | 513.095 | 12.064 | 110.573 | 312 | 750 |
| DT | Early LOP:ROP | 84 | 5.688 | 0.221 | 2.024 | 2.128 | 13.846 | 84 | 1.096 | 0.028 | 0.256 | 0.660 | 1.777 |
| DE | Flowering time | 84 | 78.238 | 0.892 | 8.180 | 62 | 91 | 79 | 77.722 | 1.062 | 9.441 | 60 | 99 |
| FC | Panicle length | 84 | 20.428 | 0.335 | 3.069 | 10.082 | 31.017 | 84 | 19.046 | 0.252 | 2.306 | 15.152 | 25.9 |
| FC | Bulk straw wt | 84 | 277.653 | 11.865 | 108.747 | 0 | 970.114 | 84 | 129.196 | 5.463 | 50.072 | 0 | 228.715 |
| FC | Bulk filled grain wt | 84 | 265.219 | 13.793 | 126.416 | 0 | 646.677 | 84 | 27.313 | 3.106 | 28.471 | 0 | 99.193 |
| FC | Harvest index | 84 | 0.468 | 0.011 | 0.101 | 0 | 0.662 | 84 | 0.138 | 0.013 | 0.123 | 0 | 0.388 |

DA, drought avoidance; DT, drought tolerance; DE, drought escape; FC, fitness component; SDW, shoot dry weight; rXSE, relative xylem sap exudation; aXSE, absolute XSE; LOP:ROP, leaf:root osmotic potential.

Baseline and drought-induced transcript expression show genetic variation

We then selected a mini-core of six rice accessions to assess genome-wide gene expression. This mini-core represented the major subgroups of rice that contain accessions from drought-prone deepwater, rainfed lowland and upland agro-ecosystems: tropical japonica (Azucena), indica (Cong Liang 1, IR64 and Kinandang Puti), and *circum-aus* (Bhadoia 303 and Kasalath). The indica accessions come from different subgroups and agro-ecosystems (Supplemental Dataset S1). The *circum-aus* accessions respond differently to variation in water availability: Bhadoia 303 shows excellent flooding tolerance as an accession with the SNORKEL1 and -2 haplotypes (Dwivedi et al., 1992; Hattori et al., 2009). Kasalath has the “reference” *SUB1A*, -B, and -C haplotypes of the submergence-tolerant accession FR13A, and these alleles alter patterns of submergence and drought tolerance (Xu et al., 2006; Fukao et al., 2011; Singh et al., 2020).

We measured transcript levels from leaf blades and crown root tips of four biological replicate plants per genotype per field at 32 days after seedling transplant, and 14 days after withholding water in the dry field, using a liquid automation-based 3'-mRNA-seq quantification approach (Supplemental Data Set S5; Groen et al., 2020). After filtering out rarely expressed transcripts (expressed in <10% of shoot or root samples) we included 21,060 shoot transcripts, and 22,707 root transcripts in our analyses (Supplemental Data Sets S6 and S7).

A principal component analysis (PCA) of all transcripts across all samples revealed a high similarity among the four biological replicates within each genotype × tissue × environment combination. A clear separation between shoot and root samples was observed on the first principal

component (PC1), explaining 41% of the total variance ($P = 6.64 \times 10^{-119}$; Supplemental Figure S3A and Supplemental Data Set S8). As expected, the most enriched gene ontology (GO) biological process on PC1 was “Photosynthesis” ($P = 3.00 \times 10^{-29}$; Supplemental Figure S3). Field environment was correlated with PC2, explaining 3% of the total variance ($P = 5.28 \times 10^{-14}$; Supplemental Data Set S8), whereas genotype was the third-most important factor, correlating with PC3 ($P = 4.67 \times 10^{-4}$; Supplemental Figure S3A).

Separating the data per tissue revealed a mild effect of drought on the shoot transcriptome: we observed 86 differentially expressed genes (DEGs; \log_2 fold change > |1|, FDR $q < 0.05$) across the mini-core accessions. Of these, 44 were upregulated and 42 were downregulated after water limitation, while we did not identify unique DEGs for individual accessions (Figure 2; Supplemental Data Set S9). Among GO biological processes enriched among shoot DEGs was the pentose-phosphate shunt (Supplemental Data Set S9), which generates nicotinamide adenine dinucleotide phosphate for reductive synthesis as well as intermediate metabolites for a range of biosynthetic processes (Hou et al., 2007). Pentose-phosphate shunt genes, including 6-PHOSPHOGLUCONATE DEHYDROGENASE2 (*Os6PGDH2*, *Os11g0484500*), are known to be responsive to drought and other abiotic stresses (Hou et al., 2007).

In contrast to the shoot transcriptome, drought had a much more pronounced effect on the root transcriptome, as reflected by the much higher number of up- and downregulated DEGs (2,158 and 430, respectively) across accessions (Figure 2B; Supplemental Data Set S10). Individual accessions further varied in the number of drought-responsive DEGs in their roots (Supplemental Figure S4 and Supplemental Data

Table 2 Quantitative genetic partitioning of variation and significance of effects across dry and wet environments for each trait

| Type | Trait | Random effects | | | Fixed effects | | | Resid. | E | F value | P value | H^2 ^a |
|------|----------------------|----------------|---------|-------------|---------------|---------|-------------|---------|-----------|----------|-------------|--------------------|
| | | G | F value | P value | G × E | F value | P value | | | | | |
| DA | Early SDW | 0.251 | 0.96 | 0.5128 | 0.176 | 0.67 | 0.8462 | 0.262 | 23.626 | 90.36 | 2.20E-16*** | 0.68 |
| DA | Late SDW | 17.641 | 2.53 | 0.0009*** | 3.758 | 0.54 | 0.9441 | 6.963 | 20.107 | 2.89 | 0.0917 | 0.87 |
| DA | Early rXSE | 0.332 | 1.73 | 0.0361* | 0.310 | 1.62 | 0.0578 | 0.191 | 7.762 | 40.59 | 3.27E-09*** | 0.65 |
| DA | Late rXSE | 0.406 | 1.89 | 0.0188* | 0.244 | 1.13 | 0.3250 | 0.215 | 65.722 | 305.53 | 2.00E-16*** | 0.73 |
| DA | Early aXSE | 0.698 | 1.69 | 0.0426* | 0.522 | 1.27 | 0.2134 | 0.412 | 11.043 | 26.79 | 8.78E-07*** | 0.69 |
| DA | Late aXSE | 6.89 | 1.61 | 0.0603 | 4.95 | 1.16 | 0.3037 | 4.28 | 1,301.15 | 303.84 | 2.00E-16*** | 0.7 |
| DA | Stem width | 0.012 | 11.72 | 2.20E-16*** | 0.003 | 2.54 | 0.0009*** | 0.0011 | 0.121 | 114.54 | 2.20E-16*** | 0.89 |
| DA | Tiller nr | 41.54 | 5.46 | 8.56E-10*** | 18.19 | 2.39 | 0.0019** | 7.61 | 745.93 | 98.01 | 2.20E-16*** | 0.81 |
| DA | Crown root nr | 14,562 | 3.32 | 2.13E-05*** | 12,416 | 2.83 | 0.0002*** | 4,392 | 2,650,813 | 603.49 | 2.20E-16*** | 0.68 |
| DA | Crown root density | 10 | 1.60 | 0.0612 | 12.56 | 2.02 | 0.0105* | 6.23 | 494.16 | 79.29 | 4.97E-15*** | 0.59 |
| DT | Early LOP | 3,175.8 | 0.95 | 0.5312 | 3,961 | 1.18 | 0.2825 | 3,356.6 | 11,356.8 | 3.38 | 0.0683 | 0.57 |
| DT | Early ROP | 6,630 | 1.02 | 0.4422 | 6,555 | 1.01 | 0.4554 | 6,489 | 7,519,672 | 1,158.75 | 2.20E-16*** | 0.62 |
| DT | Early LOP:ROP | 1.24 | 0.53 | 0.948 | 1.33 | 0.57 | 0.9256 | 2.33 | 885.54 | 379.42 | 2.20E-16*** | 0.56 |
| DE | Flowering time | 552.72 | 64.70 | 2.20E-16*** | 21.23 | 2.49 | 0.0012** | 8.54 | 3.25 | 0.38 | 0.5387 | 0.98 |
| FC | Panicle length | 42,431 | 23.39 | 2.20E-16*** | 7,295 | 4.02 | 6.94E-07*** | 1.814 | 80.157 | 44.19 | 8.11E-10*** | 0.92 |
| FC | Bulk straw wt | 15,435 | 2.87 | 0.0002*** | 10,129 | 1.88 | 0.0191* | 5,384 | 9,25,661 | 171.93 | 2.20E-16*** | 0.73 |
| FC | Bulk filled grain wt | 22,163 | 6.28 | 2.32E-11*** | 25,274 | 7.16 | 5.68E-13*** | 3,532 | 2,377,164 | 673.12 | 2.20E-16*** | 0.63 |
| FC | Harvest index | 0.023 | 3.67 | 3.78E-06*** | 0.042 | 6.72 | 3.48E-12*** | 0.006 | 4.561 | 728.23 | 2.20E-16*** | 0.51 |

DA, drought avoidance; DT, drought tolerance; DE, drought escape; FC, fitness component ($n = 168$); SDW, shoot dry weight; rXSE, relative xylem sap exudation; aXSE, absolute XSE; LOP:ROP, leaf:root osmotic potential; G, genotype; G × E, genotype × environment; Resid., residual; E, environment; H^2 , broad-sense heritability.

^aBroad-sense heritability (H^2) was calculated as described in the "Materials and methods".

Set S11), with the deepwater *circum*-aus accession Bhadoia 303 from Bangladesh showing the largest number (841 induced and 239 repressed transcripts; Supplemental Figure S4A), and the rainfed lowland indica accession Cong Liang 1 from China the lowest (442 induced and 152 repressed transcripts; Supplemental Figure S4C). These transcriptomic differences might be reflective of known differences in root anatomy and physiology between accessions. For example, lateral root branching in response to drought varies among rice genotypes (Kano et al., 2011; Catolos et al., 2017), and stele and xylem vessel structure as well as sclerenchyma development show genotypic variation (Kondo et al., 2000). Rice varieties further differ in patterns of hydraulic conductivity (Henry et al., 2012; Grondin et al., 2016), as we have measured in our diversity panel (Figure 1D).

To identify which root transcriptional changes constitute a drought response that is conserved across rice subgroups, we classified root DEGs either as shared between accessions or as unique. We observed that the largest group of shared DEGs was the one consisting of DEGs that all accessions had in common, while much smaller numbers of DEGs were shared between subsets of accessions (Figure 2C; Supplemental Data Set S11). Among the shared root DEGs we observed an enrichment of biological processes involved in responses to changing water availability such as ones related to ABA signaling and carboxylic acid metabolism (Figure 2D; Supplemental Data Set S11). Carboxylic acids (especially citric acid) are frequently detected in root exudates and may be able to mobilize phosphorus and other diffusion-limited nutrients that become less available as the soil dries (Gerke, 1995). More unexpectedly, we also found enrichment of processes related to changes in biotic interactions, including interactions with fungi (Figure 2D; Supplemental Data Set S11). Nutrient uptake under drought

may be facilitated further through plant interactions with fungi such as AMF (Lanfranco et al., 2018).

We went on to apportion transcript level variance to its sources, so that we could get an impression of the heritability of gene expression patterns. As expected, there was more transcript variation in roots than in shoots, and water availability explained a larger proportion of variance for roots. However, it was surprising to see that genotype explained a similar proportion of transcript variation in both tissues. Among the shoot samples, PC1 explained 8% of the total variance and was correlated with water availability ($P = 7.96 \times 10^{-7}$), while PC2 explained 5% of the total variance and was correlated with genotype ($P = 2.78 \times 10^{-34}$; Figure 2E; Supplemental Data Set S8). Among the root samples, PC1 explained 22% of the total variance and was correlated with water availability ($P = 4.09 \times 10^{-27}$), while PC2 explained 4% of the total variance and was correlated with genotype ($P = 3.13 \times 10^{-10}$; Figure 2F; Supplemental Data Set S8).

Shoot and root transcript modules correlate with adaptive drought resistance traits

To identify functional gene expression clusters, i.e. transcript modules of highly co-expressed genes across plants in the wet and dry environments, we ran weighted gene co-expression network analysis (WGCNA) for the shoots and roots separately (Supplemental Figure S5; Langfelder and Horvath, 2008). We identified 55 and 112 modules across all shoot and root transcripts, respectively. Of these, 17 shoot and 20 root modules together contained most transcripts (Figures 3 and 4; Supplemental Figure S6 and Supplemental Data Set S12). We focused on these modules for further analysis and calculated the eigengene for each module. The eigengene is the first principal component of a co-expression

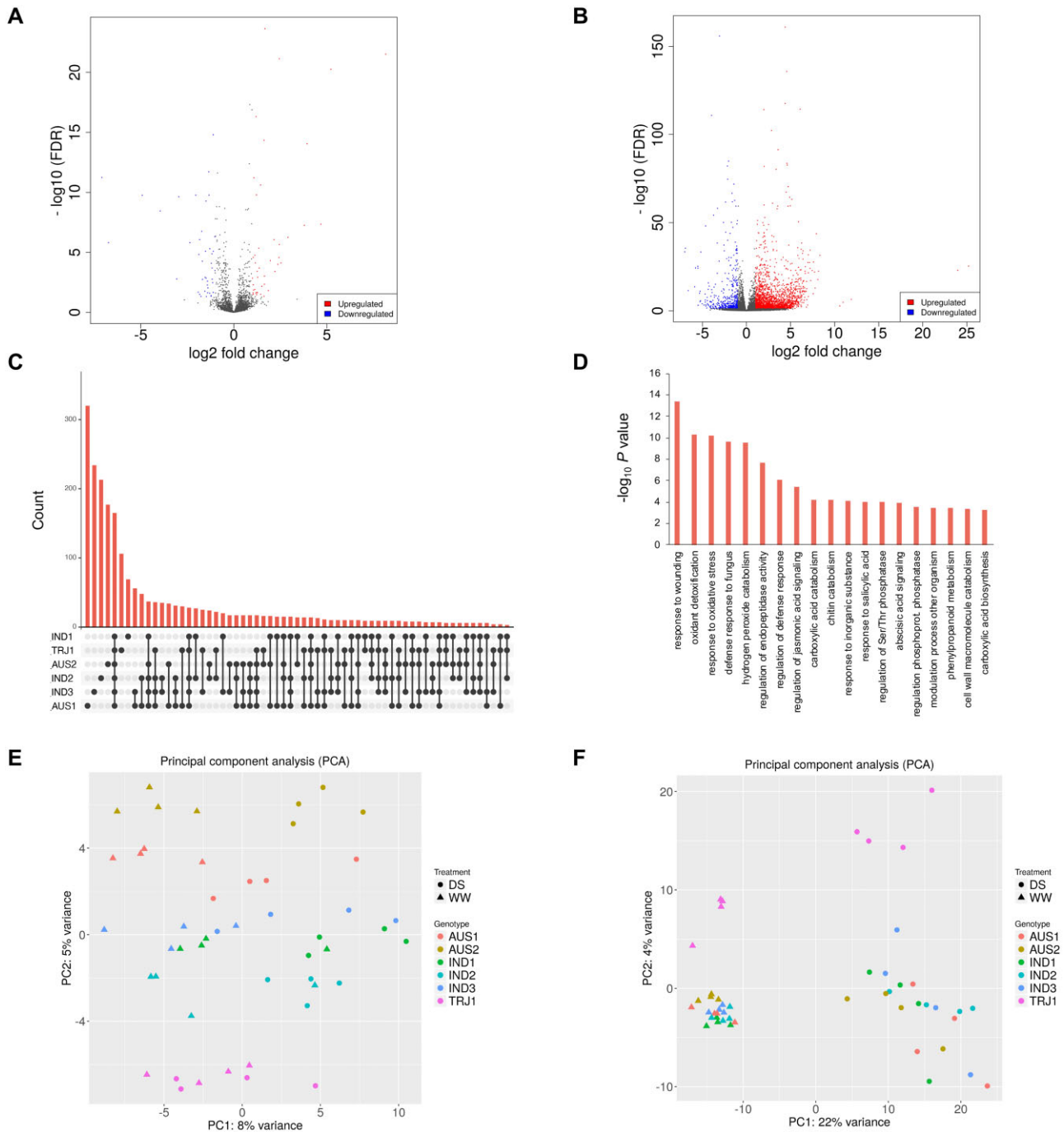


Figure 2 Drought-induced root transcriptional responses were stronger and more accession-specific than shoot responses. **A**, The number of DEGs in rice shoot samples (leaf blades) across accessions between wet and dry conditions ($FDR\ q < 0.05$). **B**, The number of DEGs in crown root tips under water limitation across accessions ($FDR\ q < 0.05$). **C**, The UpSet plot shows the number of root DEGs (y -axis) that were unique for each accession or shared between subsets or all of the accessions. **D**, Enrichment of GO biological processes among the drought-induced root DEGs shared between all accessions (y -axis shows $-\log_{10}$ of $P < 0.05$). **E**, PCA on the gene expression data shows that PC1 largely separates leaf samples by wet and dry conditions and PC2 largely separates these by accession ($n = 48$). **F**, Root transcriptome samples separated more clearly by environment along PC1 than shoot samples, while only the roots of the tropical japonica accession Azucena clearly separated from the indica and *circum-aus* accessions along PC2 ($n = 48$). Abbreviations: WW = well-watered (wet) conditions; DS = dry spell (dry) conditions; AUS1 and AUS2 = *circum-aus* accessions Bhadoia 303 (salmon) and Kasalath (gold), respectively; IND1, IND2, and IND3 = indica accessions Cong Liang 1 (green), IR64 (cyan), and Kinandang puti (blue), respectively; TRJ1 = tropical japonica accession Azucena (pink).

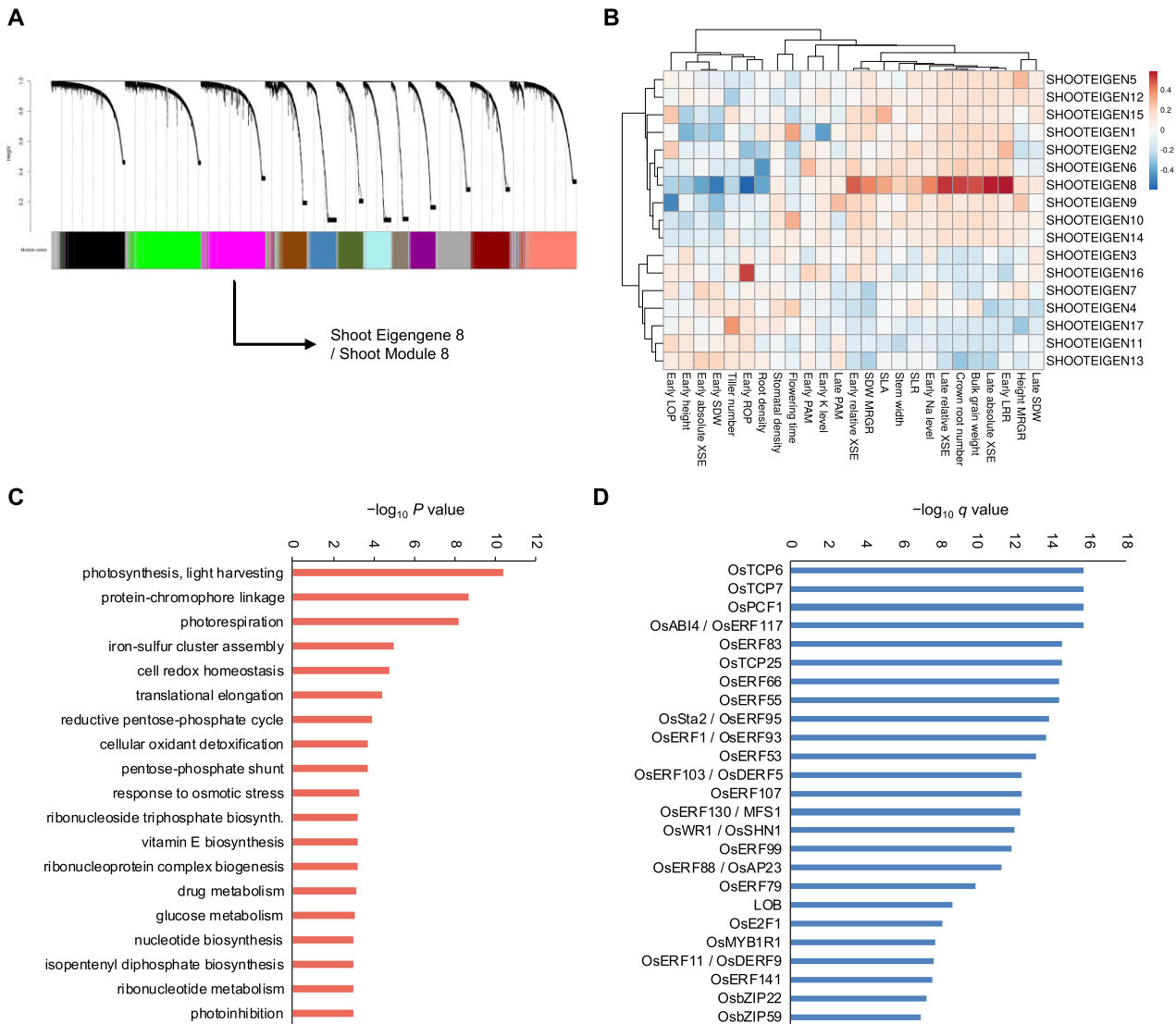


Figure 3 A fitness-linked shoot co-expression module is involved in photosynthesis and regulated by drought-responsive TFs. A, WGCNA identified 17 shoot gene co-expression modules that together represented over 50% of all transcripts included in our analyses. B, The heatmap shows Pearson product-moment correlation coefficients between the baseline (constitutive) trait values of each replicate plant for every trait (including the fitness component bulk filled grain weight) in each environment and the loadings of each replicate plant per environment onto the eigengene (PC1) for each of the 17 shoot gene co-expression modules. Correlations with the fitness component bulk filled grain weight were considered significant when Bonferroni-adjusted $P < 3.46 \times 10^{-4}$ ($n = 48$). C, GO biological processes enriched for shoot module 8 (y-axis shows $-\log_{10}$ of $P < 0.05$). D, Enrichment of binding sites for TFs among promoters of transcripts in module 8 (y-axis shows $-\log_{10}$ of FDR $q < 0.05$).

module and reflects the expression trends of all member transcripts of that module (Langfelder and Horvath, 2008). We then looked for correlations between transcript module eigengenes and fitness as well as fitness-associated traits.

The eigengenes of shoot module 8, as well as root modules 1 and 11, were the only three eigengenes that strongly correlated with fitness (filled grain yield) across environments (Bonferroni-adjusted $P < 3.46 \times 10^{-4}$ and $P < 2.50 \times 10^{-4}$ for shoots and roots, respectively; Supplemental Data Sets S13 and S14). They also showed significant correlations with all fitness-associated traits: the drought-avoidance traits absolute xylem sap exudation (early and late) and root density, and the drought-tolerance traits Ψ_{leaf} , Ψ_{root} , and $\Psi_{\text{leaf/root}}$

($P < 0.05$, except for the correlation between shoot module 8 and Ψ_{leaf} for which $P = 0.0852$; Figures 3 and 4; Supplemental Data Sets S13 and S14). Important from evolution and breeding perspectives, all three modules showed robust heritability with $H^2 \geq 0.7436$ (Supplemental Data Set S15).

A drought-adaptive shoot transcript module is linked to plant growth

To gain more insights into the biological roles of the transcript modules associated with drought-adaptive traits, we analyzed whether the modules correlated with additional drought avoidance and tolerance traits that we were able to

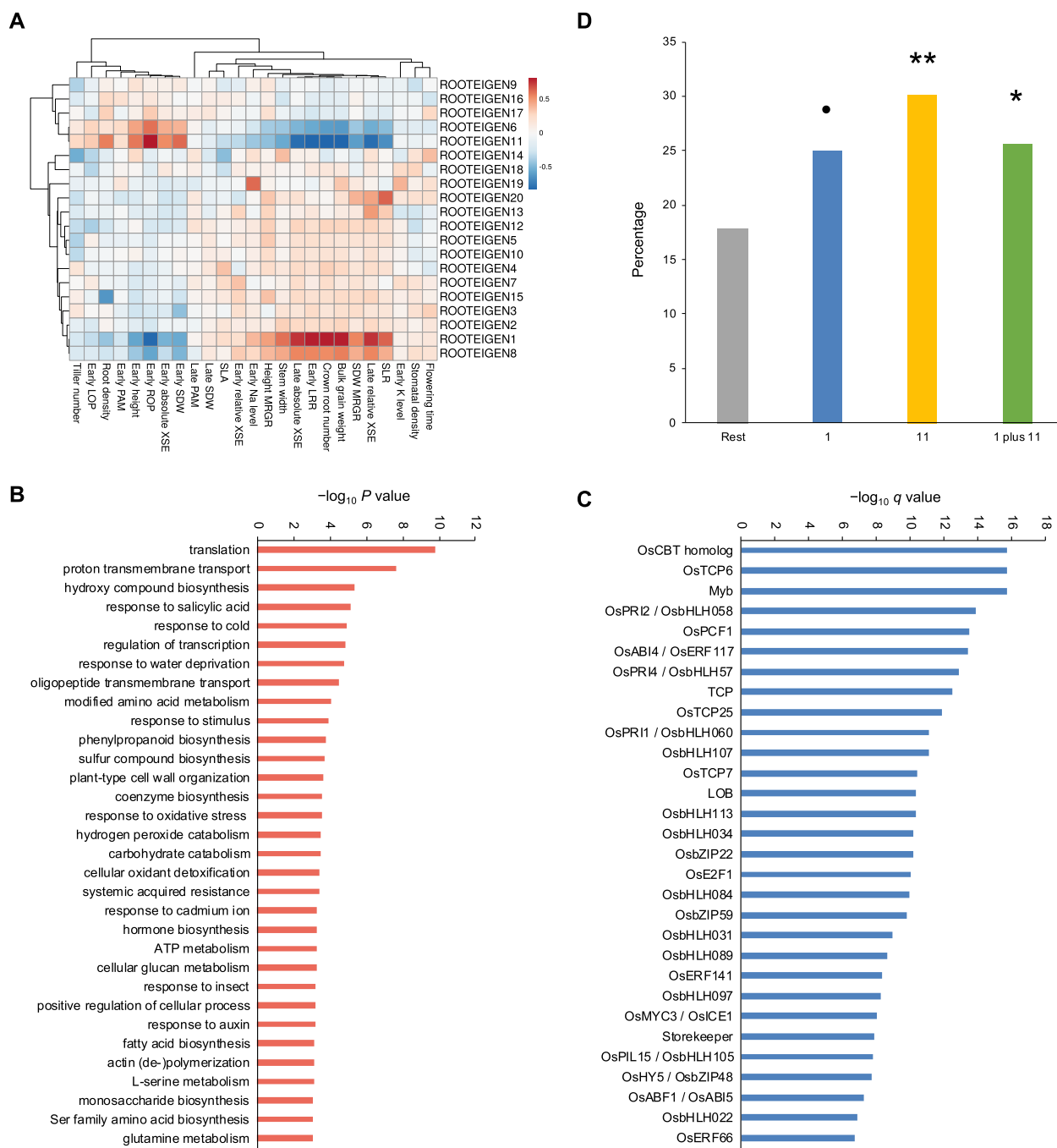


Figure 4 Two fitness-linked root co-expression modules integrate responses to changing abiotic and biotic factors under drought. A, The heatmap shows Pearson product-moment correlation coefficients between the baseline (constitutive) trait values of each replicate plant for every trait (including the fitness component bulk filled grain weight) in each environment and the loadings of each replicate plant per environment onto the eigengene (PC1) for each of the 20 root gene co-expression modules identified through WGCNA. The 20 modules together represented over 50% of all transcripts included in our analyses. Correlations with the fitness component bulk filled grain weight were considered significant when Bonferroni-adjusted $P < 2.50 \times 10^{-4}$ ($n = 48$). B, GO biological processes enriched for root module 1 (y -axis shows $-\log_{10}$ of $P < 0.05$). C, Enrichment of binding sites for TFs among promoters of transcripts in module 1 (y -axis shows $-\log_{10}$ of FDR $q < 0.05$). D, Enrichment of crown root tip transcripts that were differentially regulated in response to interaction with AM fungi in [Gutjahr et al. \(2015\)](#) among root modules 1 and 11. Notation of significance for χ^2 test: ** $P < 0.01$, * $P < 0.05$, $P < 0.1$.

measure for the mini-core panel. These included the avoidance traits (1) early shoot height, (2) late shoot dry weight, (3) shoot relative growth rates (RGRs, based on height and

dry weight), (4) stem-to-leaf ratio, (5) specific leaf area, (6) stomatal density, and (7) chlorophyll fluorescence (early and late). They also included the tolerance traits xylem sap

sodium (Na^+) and potassium (K^+) content (Supplemental Data Set S13).

Shoot module 8, as well as root modules 1 and 11, all correlated with the drought tolerance trait xylem sap sodium (Na^+) content ($P \leq 0.0089$), and the drought avoidance trait shoot RGR based on dry weight ($P \leq 0.0053$; Figures 3 and 4; Supplemental Data Sets S13 and S14). In addition, shoot module 8 and root module 11 correlated with specific leaf area (SLA; $P \leq 0.0292$), while root modules 1 and 11 further correlated with early shoot height ($P \leq 1.66 \times 10^{-5}$), shoot RGR based on height ($P \leq 0.0013$), and stem-to-leaf ratio ($P \leq 1.82 \times 10^{-6}$; Figures 3 and 4).

Shoot module 8 correlated with growth-related morphological traits, as reflected in shoot dry weight-based RGR and SLA (Figure 3B), and in addition with water spending-related physiological traits, as reflected in absolute xylem sap exudation (early and late), Ψ_{root} , and $\Psi_{\text{leaf/root}}$ (Figure 3B). Growth is in part fueled by photosynthesis and involves increasing both physical size and protein synthesis (Kleessen et al., 2014). Indeed, shoot module 8 was enriched for photosynthesis- and translation-related GO biological processes and we will refer to this module as the “photosynthesis module” (Figure 3C; Supplemental Data Set S16).

The photosynthesis module was further enriched in promoter elements targeted by TEOSINTE BRANCHED1/CYCLOIDEA/PROLIFERATING CELL FACTOR (TCP) and APETALA2/ETHYLENE RESPONSE FACTOR (AP2/ERF) TFs (Figure 3D; Supplemental Data Set S16). TCPs are regulators of cell proliferation (Yao et al., 2007), while AP2/ERF TFs such as ABA-INSENSITIVE4 (OsABI4/OsERF117, Os05g0351200) and WAX SYNTHESIS REGULATORY GENE1 (OsWR1/OsSHN1/OsERF3, Os02g0202000) are involved in abiotic stress signaling. Upon drought perception, OsABI4 and OsWR1 transcriptionally activate processes such as protective epicuticular wax production (Wang et al., 2012; Mukhopadhyay and Tyagi, 2015). Other TF binding sites with enrichment included sites for BASIC LEUCINE ZIPPER22 (OsZIP22, Os02g0728001), E2 PROMOTER-BINDING FACTOR F1 (OsE2F1, Os02g0537500), and MYELOBLASTOSIS1REPEAT1 (OsMYB1R1, Os01g0192300; Figure 3D). These TFs previously emerged as key regulators of dehydration response- and photosynthesis-related genes in an environmental gene regulatory influence network (Wilkins et al., 2016).

Two drought-adaptive root modules integrate responses to abiotic and biotic changes

Like the photosynthesis module, root modules 1 and 11 correlated with growth-related morphological traits as well (Figures 3 and 4). In addition, they were tied to the drought avoidance traits absolute xylem sap exudation (early and late) and root density, which relate to a water-spending strategy. The two root modules were further correlated with the drought tolerance traits Ψ_{leaf} , Ψ_{root} , $\Psi_{\text{leaf/root}}$, and xylem sap sodium (Na^+) content, which are involved in osmotic adjustment (Chen and Jiang, 2010). These molecular

and physiological root traits may be intricately related to phenotypic shoot alterations in response to water limitation. Shoot growth and development depend on a sufficient supply of water coming from the root system, since water spending is a prerequisite for photosynthesis (Calvin, 1956). This supply can be promoted by appropriate values of $\Psi_{\text{leaf/root}}$ and Ψ_{root} (Turner, 2018). Another mechanism known to contribute to water supply to the shoot is root expression of aquaporins (Sakurai et al., 2008; Henry et al., 2012; Grondin et al., 2016). Transcripts from 28 of 34 known aquaporin genes were expressed in our crown root samples (Supplemental Data Set S17; Nguyen et al., 2013; Sakurai et al., 2005). Root modules 1 and 11, which were not only correlated with plant fitness, but also with xylem sap exudation, were significantly enriched for these aquaporin transcripts (χ^2 test, $P = 0.019$; Supplemental Data Set S17). This suggests that root aquaporin expression could contribute to fitness under drought by controlling the water supply to the shoot as measured by xylem sap exudation.

Root module 1 was further enriched for the GO biological processes “response to water deprivation”, “response to hypoxia”, “cellular response to phosphate starvation”, and several metabolism-related processes (Figure 4B; Supplemental Data Set S17). We will refer to this module as the “root drought module” since these processes seem to reflect differences between soils in the wet and dry fields. The processes enriched in the root drought module may also be functionally linked to several of the drought avoidance and tolerance traits to which this module was positively correlated: late absolute and relative xylem sap exudation, late crown root number, and $\Psi_{\text{leaf/root}}$. In relation to its enrichment for “cellular response to phosphate starvation”, the root drought module was further enriched for “carboxylic acid metabolism” (Figure 4B), a process that may help to mobilize sources of P (Gerke, 1995).

One of the factors that may explain why genes responsive to drought and phosphate starvation make an outsized contribution to between-accession expression differences in root drought module transcripts is that our mini-core harbors natural genetic variation for possession of the protein kinase PHOSPHORUS-STARVATION TOLERANCE1 (PSTOL1; Chin et al., 2011). For example, PSTOL1 is expressed in the *circum*-aus accession Kasalath, but not in the indica accession IR64 or the reference-genome japonica accession Nipponbare (Chin et al., 2011; Gamuyao et al., 2012). When active, PSTOL1 confers enhanced tolerance to P deficiency, and genes regulated by PSTOL1 activity in *Pro35S:PSTOL1*_{Kasalath}-transgenic IR64 plants co-localize with root and drought quantitative trait loci (Gamuyao et al., 2012). Strikingly, we observed that the root drought module was indeed enriched for PSTOL1-regulated genes (χ^2 test, $P = 0.0135$; Supplemental Data Set S17).

In addition, root drought module transcripts were regulated more often than expected by chance by the same TCP and OsABI4/OsERF117 TFs that we observed for the photosynthesis module (Figure 4C; Supplemental Data Set S17).

There was also a signature of regulation by the TF ABA-RESPONSIVE ELEMENT-BINDING FACTOR1 (OsABF1/OsABI5/OsbZIP10, Os01g0867300; Figure 4C), which has known roles in regulating rice responses to water deprivation (Zou et al., 2008; Hossain et al., 2010; Zhang et al., 2017). Compared to the photosynthesis module and root module 11, the root drought module was uniquely defined by enrichment for basic HELIX–LOOP–HELIX TFs, including POSITIVE REGULATORS OF IRON HOMEOSTASIS (OsPRIs), as well as by enrichment of TF activity by a CALMODULIN-BINDING TRANSCRIPTION FACTOR homolog, encoded by Os03g0191000 (Figure 4C). The latter is a positive regulator of responses to abiotic stress and a negative regulator of biotic interactions (Prasad et al., 2016). OsPRIs regulate root and shoot responses to deficiencies in micronutrients such as iron (Kobayashi et al., 2019; Li et al., 2020).

Root module 11 was enriched for GO biological processes that include “carboxylic acid metabolism”, which was also seen as enriched in the root drought module, “response to fungus”, and processes related to oxidative stress responses (Supplemental Figure S6B and Supplemental Data Set S17). This module was strongly linked with root density ($P = 4.47 \times 10^{-5}$), and, compared to the photosynthesis and drought modules, was uniquely enriched for the activity of NO APICAL MERISTEM/ARABIDOPSIS TRANSCRIPTION ACTIVATION FACTOR/CUP-SHAPED COTYLEDON (NAC) TFs (Supplemental Figure S6C and Supplemental Data Set S17). One of these TFs was OsNAC2 (Os04g0460600), which is a known regulator of root development, including crown root number (Mao et al., 2020).

Upon closer examination, it was not only root module 11 that was enriched for processes known to be associated with interactions between plant roots and fungi such as AMF. The root drought module was enriched for such processes as well (Figure 4B; Supplemental Figure S6B), including peptide transport, cell wall organization, and signaling by phytohormones such as auxin and salicylic acid (Gutjahr and Paszkowski, 2009; Gutjahr et al., 2015). Furthermore, the root drought module and root module 11 were enriched for transcripts that are differentially expressed in crown roots upon interaction with AMF (Gutjahr et al., 2015). Of transcripts in these modules, 25.6% were AMF-responsive DEGs compared to 17.9% of transcripts in the rest of the genome ($P = 0.0427$; Figure 4D; Supplemental Data Set S18). This enrichment was driven in particular by root module 11, of which 30.1% of transcripts were also AMF-responsive DEGs ($P = 0.0014$; Figure 4D), and we will refer to this module as the AMF interactions module.

We detected expression of late-stage symbiosis marker genes in 25% of our nodal root samples (Gümil et al., 2005; Gutjahr et al., 2008), with a slight enrichment for plants in dry versus wet conditions (Fisher’s exact test, $P = 0.0496$, Supplemental Data Set S18). This was despite the fact that we measured gene expression at an early stage after the start of soil drying relative to previously observed progression in the establishment of root interactions with AMF,

and that we sampled nodal roots, which are typically not colonized as strongly as large lateral roots (Gutjahr et al., 2009; Fiorilli et al., 2015). Among the marker genes were PHOSPHATE TRANSPORTER11 (OsPT11, Os01g0657100; Yang et al., 2012a), STUNTED ARBUSCULE2 (OsSTR2, Os07g0191600; Gutjahr et al., 2012), ARBUSCULAR MYCORRHIZAL MARKER25 (OsAM25, Os06g0552700; Fiorilli et al., 2015), and OsAM34 (Os10g0332000; Gutjahr et al., 2008; Fiorilli et al., 2015), and expression of these was accompanied by relatively frequent expression of common symbiosis marker genes. The latter did not show enriched expression in dry conditions (Fisher’s exact test, $P = 0.6259$, Supplemental Data Set S18), as expected (Gutjahr et al., 2008). Interestingly, at this relatively early stage we observed marker gene expression in the indica and japonica accessions, but not in the *circum-aus* accessions, which agrees with published patterns of genetic diversity for mycorrhizal symbiosis in rice (Jeong et al., 2015).

Overall, the transcriptome data suggest that the fitness-associated root drought and AMF interaction modules are not only enriched for transcripts from genes known to be involved in plant responses to drought. They are also enriched for transcripts from genes that mediate root interactions with AMF. This brings up the hypotheses that drought may alter plant–fungus interactions and that AMF may have an effect on plant fitness in water-limited environments. We will elaborate further on these possibilities below.

Evidence of polygenic selection on fitness-associated transcript modules

Next, we wished to explore if the modules of co-expressed transcripts linked to fitness would show evidence of polygenic selection among rice varieties that regularly experience drought versus rice varieties that do not. One approach was to analyze if genomic regions encoding transcripts within these modules show cumulative effects of differential selection relative to genomic regions encoding the leaf- and root-expressed transcripts outside of these modules. Differential selection may be signified by higher levels of F_{ST} , a measure of genetic divergence between groups of individuals (Hämälä et al., 2020; Campbell-Staton et al., 2020). Among rice subgroups, temperate japonica accessions are almost exclusively grown in irrigated agro-ecosystems, whereas *circum-aus*, indica, and tropical japonica accessions (including ones in our mini-core) are also grown frequently in drought-prone rainfed systems (Gutaker et al., 2020). We therefore hypothesized that drought-adaptive genome regions should exhibit a tendency to diverge faster between the latter subgroups and temperate japonica than other genome regions.

When we conducted this analysis of polygenic selection we indeed observed above-average levels of F_{ST} between temperate japonica accessions and both the *circum-aus* and the indica accessions in genomic regions encoding the transcripts of fitness-linked co-expression modules compared to

genomic regions encoding other transcripts (Welch's t test, *indica*: $t = 1.9944$, one-tailed $P = 0.0231$; *circum-aus*: $t = 2.3723$, one-tailed $P = 0.0089$; Figure 5A; Supplemental Data Set S19). Divergence of these genomic regions was not elevated for tropical compared to temperate japonica accessions, although a trend in this direction was visible (Welch's t test, $t = 1.3511$, one-tailed $P = 0.0884$; Figure 5A). When we focused on regions that showed high F_{ST} (≥ 0.7) in all three of these comparisons, we found one region on chromosome 3 (among others) with genes encoding several fitness-linked transcripts that were previously shown to mediate drought resistance (Figure 5B; Supplemental Data Set S19). These included *MYELOBLASTOSIS2* (*OsMYB2*, Os03g0315400), *NICOTIANAMINE SYNTHASE2* (*OsNAS2*, Os03g0307200), and the ABA receptor-encoding *PYRABACTIN RESISTANCE1-LIKE6* (*OsPYL6*, Os03g0297600; Lee et al., 2017; Miao et al., 2018; Santosh Kumar et al., 2021; Yang et al., 2012b).

We then assessed whether other measures of selection would corroborate our observations on genetic divergence between accessions from drought-prone rainfed agro-ecosystems compared to stably wet irrigated systems. We previously developed GreenINSIGHT, which infers the fraction of nucleotide sites under selection in rice by comparing patterns of intra-species sequence polymorphism with interspecies divergence across dispersed genomic sites, relative to nearby neutrally evolving sites (Gronau et al., 2013; Joly-Lopez et al., 2020). Given that an estimated 89.1% of accessions in GreenINSIGHT's reference panel were originally collected in drought-prone rainfed agro-ecosystems (Joly-Lopez et al., 2020), we hypothesized that we would observe signatures of selection in the genomic regions from which the transcripts of the fitness-associated co-expression modules originate. We considered two selection-related parameters that GreenINSIGHT computes: ρ (the fraction of sites under any kind of selection) and τ (the fraction of polymorphisms under weak negative selection).

While we observed a trend of higher ρ scores for the genomic regions tied to the photosynthesis, root drought, and AMF interaction co-expression modules than ρ scores for genomic regions that did not code for transcripts associated with fitness in our experiment, this trend was not significant (Welch's t test, $t = 1.1177$, one-tailed $P = 0.1319$; Figure 5; Supplemental Data Set S19). However, we did observe a modestly significant pattern of more pervasive weak negative selection in the form of higher τ scores for these genomic regions (Welch's t test, $t = 1.7992$, one-tailed $P = 0.036$; Figure 5). Zooming in on regions that both encode fitness-linked transcripts and show high ρ and τ scores (> 0.9) revealed one region on chromosome 6 and two on chromosome 10 containing genes involved in regulating plant architecture and one (*Os10g0356000*) that encodes the Rubisco large subunit *OsRbcL* (Figure 5C; Supplemental Data Set S19).

Taken together, these analyses suggest that the genomic regions encoding the transcripts that are part of the fitness-associated shoot and root gene co-expression modules experience polygenic selection in the *indica* and *circum-aus*

subgroups, whose members more often inhabit drought-prone rainfed agro-ecosystems than the temperate japonica subgroup. Furthermore, weak negative or purifying selection may be more pervasive in these regions compared to other transcriptionally active genomic regions.

Transcript modules under selection reflect adaptive variation in functional traits

Patterns of enrichment for biological processes in the shoot and root transcript modules that showed adaptive variation in their behavior suggested that lower WUE and higher levels of stomatal conductance and photosynthesis might have contributed to higher fitness. In addition, the root gene expression data suggested that such photosynthesis- and fitness-related traits could be linked to root drought avoidance traits. These include xylem sap exudation and environment-responsive developmental plasticity in root density—as deduced from the inferred activity of TFs such as *OsNAC2* that influence root system architecture. For roots, our field-measured transcriptome data further suggested that there may have been changes in intensity of interactions with AMF, which might have come with fitness benefits.

We aimed to confirm if these traits could contribute to fitness by measuring them in a second field season in the dry season of 2018 (Figure 6; Supplemental Data Set S20). While light- and temperature-related factors were comparable between the two field seasons (Supplemental Figure S7), precipitation- and humidity-related factors showed differences (Figure 6B; Supplemental Data Set S21). This may explain why not all traits showed significant repeatability (Figure 6C; Supplemental Data Set S22; Wolak et al., 2012). Repeatability appeared low for biomass-related traits, including the fitness component bulk straw weight (Figure 6C). We therefore decided to consider bulk filled grain weight and bulk straw weight as separate fitness components.

In shoots, the drought avoidance traits WUE, net photosynthesis and stomatal conductance were linked to bulk grain weight ($|r| > 0.286$, $P < 0.049$; Figure 6, D–F; Supplemental Data Set S23), confirming our expectations based on the gene expression data from the previous dry season. These photosynthesis-related traits are influenced by belowground drought avoidance traits that regulate water transport to the shoots, such as root density and xylem sap exudation, and these root traits showed patterns congruent with our observations for shoots. Drought-induced plasticity in root density was again adaptive in the 2018 dry season ($r = 0.644$, $P = 0.0016$; Figure 7; Supplemental Data Set S22), despite low repeatability of root density between the 2017 and 2018 seasons (Figure 6C). Furthermore, late xylem sap exudation under drought was correlated with later measurements of net photosynthesis and stomatal conductance in both the 2017 and 2018 dry seasons (Figure 7F), highlighting the links between water transport from the soil and photosynthesis in the leaves.

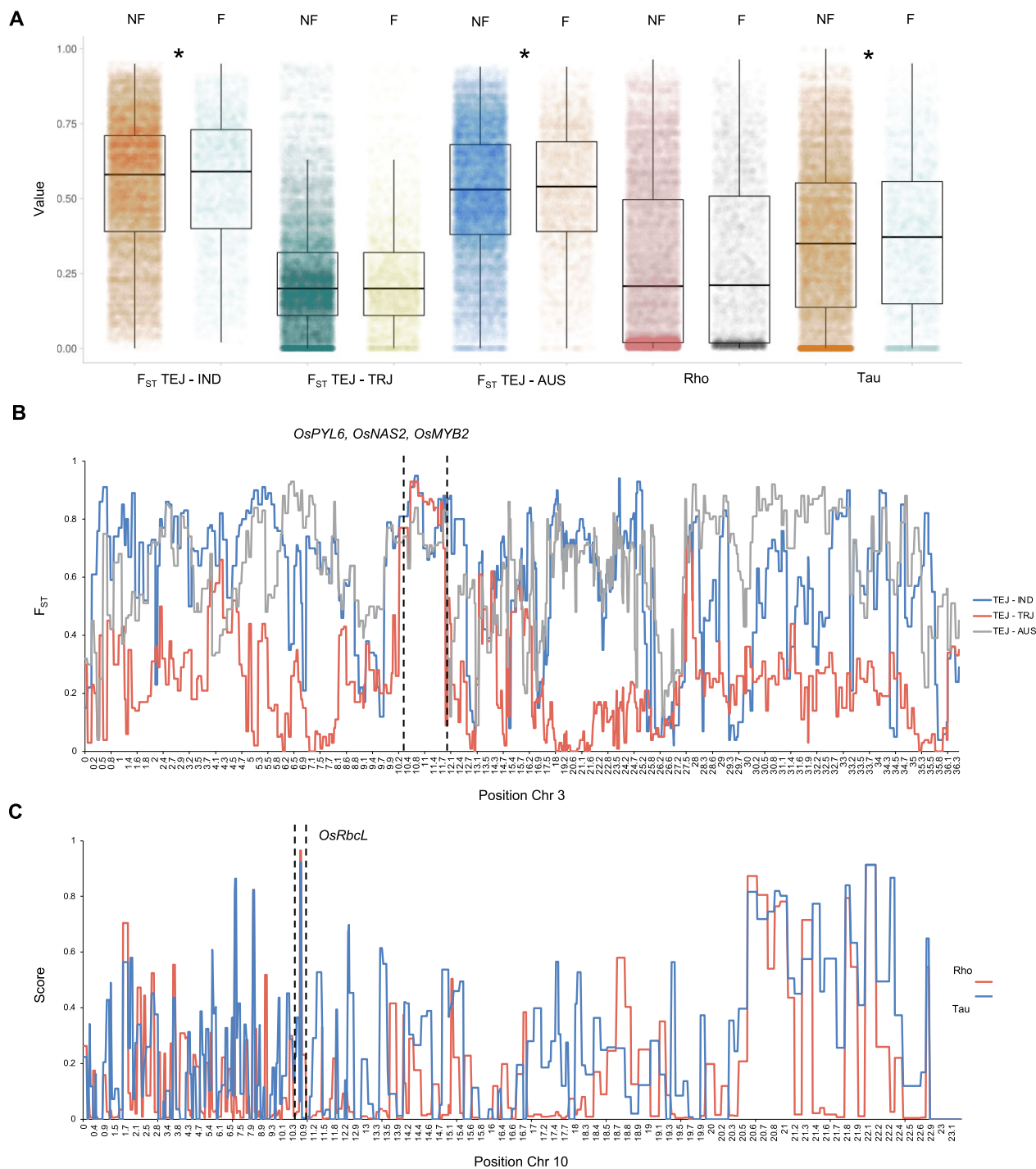


Figure 5 Fitness-linked shoot and root co-expression modules show polygenic signatures of selection across irrigated and rainfed agro-ecosystems. A, Comparison of pairwise population divergence (F_{ST}) values for the genomic regions (100-kb windows) encoding the transcripts that are part of the fitness-associated shoot and root gene co-expression modules and F_{ST} values for other transcriptionally active genomic regions in our experiment between temperate japonica accessions (TEJ)—whose members mostly inhabit stably wet irrigated agro-ecosystems—and indica (IND), circum-aus (AUS), and tropical japonica (TRJ) accessions, respectively, which are much more regularly found in drought-prone rainfed agro-ecosystems ($n = 22,954$). These regions were further compared for levels of weak negative or purifying selection (τ), and for levels of selection in general (ρ), relative to a reference population consisting predominantly of rainfed-environment accessions ($n = 22,517$). Horizontal lines denote medians, boxes delineate upper and lower quartiles, and whiskers upper and lower extremes. Notation of significance for Welch's t test: * $P < 0.05$. B, Example of a region on chromosome 3 that showed high levels of F_{ST} in all three comparisons and contained at least three genes (highlighted) that have been functionally characterized as being involved in drought resistance. C, Example of a region on chromosome 10 that showed high levels of ρ as well as τ and contained the *OsRbcL* gene (highlighted), which has an important role in photosynthesis.

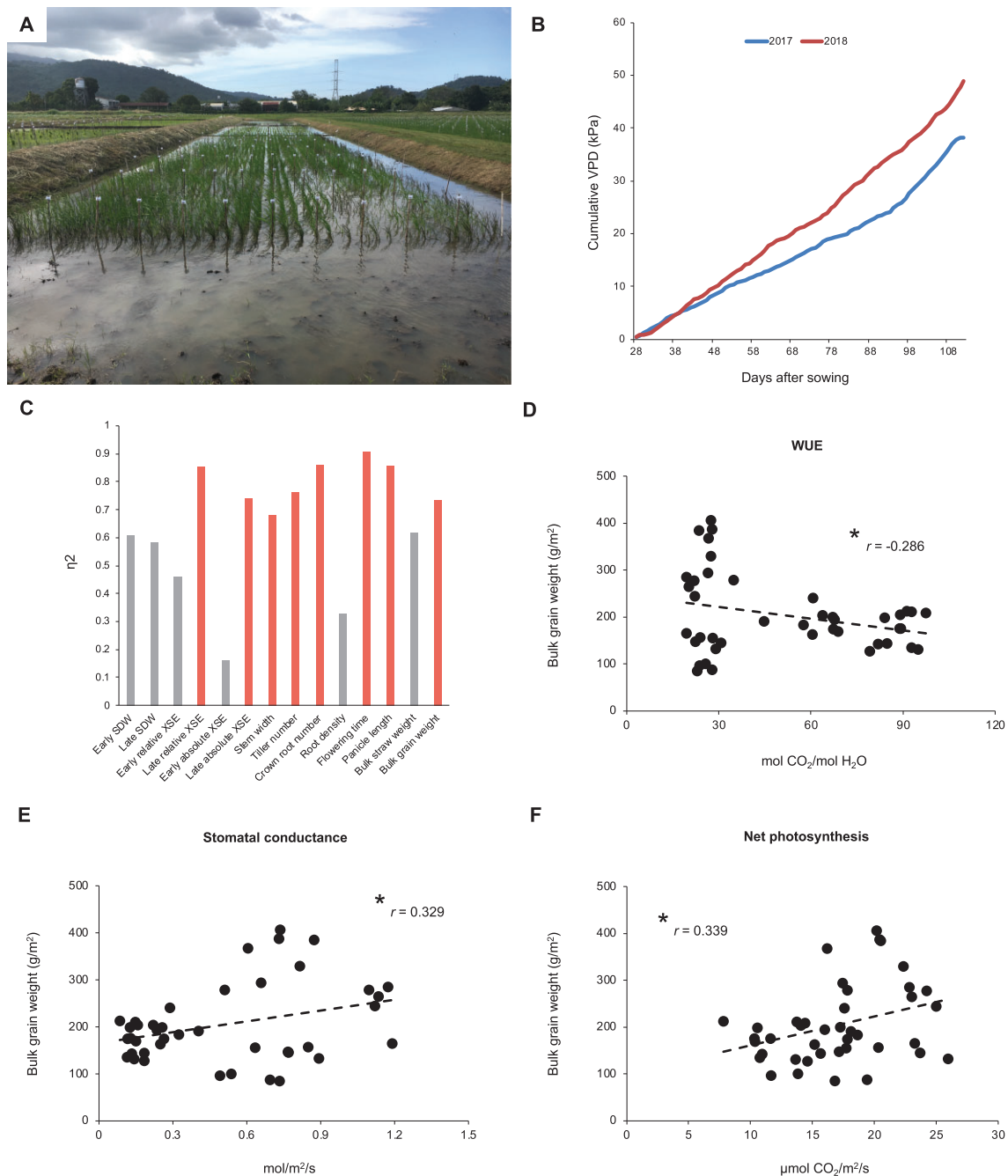


Figure 6 Gene expression patterns reflected links between leaf traits and fitness. A, The same panel of 22 rice accessions was planted in the same design in wet and intermittently dry field conditions in the 2018 dry season as it was in the 2017 dry season. The incoming clouds symbolize how weather conditions may fluctuate between days and between seasons. B, Comparison of the cumulative vapor-pressure deficit between the 2018 and 2017 dry seasons. C, Significant (red, $P < 0.05$) and nonsignificant (gray) repeatability (η^2) of drought resistance traits between the 2018 and 2017 dry seasons. D, Pearson product-moment correlation between WUE and the fitness component bulk filled grain weight ($P = 0.049$, $n = 43$) in the 2018 dry season. E, Pearson correlation between stomatal conductance and grain weight ($P = 0.0223$). F, Pearson correlation between net photosynthesis and grain weight ($P = 0.0184$). Notation of significance for Pearson's r : * $P < 0.05$.

Finally, our expectations for root traits based on the gene expression data from the 2017 field season were confirmed in 2018 as well. Levels of root interactions with AMF were tied to bulk straw weight ($r = 0.427$, $P = 0.0374$; [Figure 7C](#); [Supplemental Data Set S24](#)), particularly under drought ($r = 0.853$, $P = 0.0008$). AMF interactions may further benefit bulk filled grain weight through these effects on biomass as well, although this indirect effect was relatively weak (Estimate = 8.705, $z = 1.855$, one-tailed $P = 0.032$), as estimated through path analysis ([Rosseel, 2012](#)). Overall, these findings highlighted the power of our gene expression data as a foundation for identifying traits at higher levels of biological organization that may contribute to fitness when rice is faced with limitations in water availability.

Discussion

The evolutionary systems biology approach we opted to take in this study showed us how plants may maintain fitness under drought through integrating root and shoot physiological responses to adjust hydraulics and photosynthesis. Conducting our measurements of gene expression and physiology in the field allowed us to observe the importance of taking on board changes in biotic interactions when water conditions change to understand plant responses to drought. More field studies of such an integrative nature will need to be done to continue closing the lab–field gap ([Groen and Purugganan, 2016](#); [Zaidem et al., 2019](#)).

In our field experiment, we observed fitness associations for several traits, including xylem sap exudation and plasticity in root density as drought avoidance traits, as well as Ψ_{leaf} and plasticity in Ψ_{root} and $\Psi_{\text{leaf/root}}$ as drought tolerance traits. Although none of the tolerance traits showed strong heritability, which is a prerequisite for selection to have effects on later generations of plants, the drought avoidance traits did display robust heritability. These findings reinforce previous work showing that xylem sap exudation and root density could make valuable breeding targets, despite the fact that such root-related traits are typically harder to measure in a high-throughput manner than many aboveground traits ([Henry et al., 2016](#); [Sandhu et al., 2016](#); [Catolos et al., 2017](#)).

The latter disadvantage might be offset, however, by the fact that we observed stronger heritabilities and trait correlations with gene expression in the root traits compared to the shoot traits. Although many studies have observed the opposite, presumably since root data tends to be noisy and drought stress brings out soil heterogeneity in fields, in our study we may have measured root traits that somehow might be less error-prone than traits that have often been measured in previous studies, such as root length density at depth. Another contributing factor might be the fact that rice shoots tend to stop growing after plants have perceived water limitation during the early vegetative stage and do not show much genetic variation, whereas the roots of the genotypes that perform well under drought are quickly and

actively responding to the drought stress, thereby driving a higher degree of genetic variation.

It further seems that rice breeders have had to, and might need to continue to, work against the tendency of natural selection to promote a “water spending” strategy for this species in rainfed lowland conditions ([Tardieu and Simonneau, 1998](#)). For example, in our field study with a population that consisted mostly of landraces, xylem sap exudation rate was positively correlated to fitness under drought. However, in several previous studies with populations that contained more breeding lines and different distributions of flowering time and biomass values, the opposite pattern was observed in that drought-tolerant varieties had lower xylem sap exudation rates ([Dixit et al., 2015](#); [Henry et al., 2016](#)).

From the literature, it appears that obtaining physiological and, in particular, molecular measurements from the roots of field-grown plants is still limited by considerable practical obstacles compared to obtaining such measurements from shoots. Two published examples provide excellent insights that are extended by our study. In the first, Yu and colleagues (2018) measured gene expression in roots of field-grown maize at high and low soil phosphate levels, observing that genes involved in signaling and cell wall metabolism were particularly responsive. In the second, Kawakatsu and co-workers (2021) measured gene expression in both the roots and shoots of a panel of diverse rice accessions grown in relatively dry upland growth conditions. The upland agroecosystem is a second important rainfed system in addition to the rainfed lowland system we studied ([Wing et al., 2018](#); [Gutaker et al., 2020](#)). The authors found that genotypes showed heritable variation in root expression of genes related to auxin signaling and stress responses, and that these processes were linked with root growth characteristics ([Kawakatsu et al., 2021](#)).

Our data broadly recapitulate the main findings of these studies, while complementing them in several important ways. Not only do we include an environmental effect, but we also assessed both root and shoot tissues. Crucially, we link measurements of gene expression and physiology with measurements of fitness components, plus analyses of heritability and longer term effects of selection. That said, in our study, we were not able to include measurements of root growth at depth (i.e. beneath a 20-cm depth), which can sometimes explain a large proportion of drought responses in rice ([Henry et al., 2011](#); [Uga et al., 2013](#); [Grondin et al., 2018](#)), and can also be influenced by variation in the presence or absence of large-effect stress–response genes such as the one encoding the PSTOL1 kinase ([Gamuyao et al., 2012](#)).

Despite this limitation, we found that most of the heritable differences in environmentally sensitive gene expression between accessions could be found in the roots, pointing to the root as the primary response tissue under vegetative stage drought. While the indica accession Cong Liang 1 from China showed the lowest number of DEGs (594 root

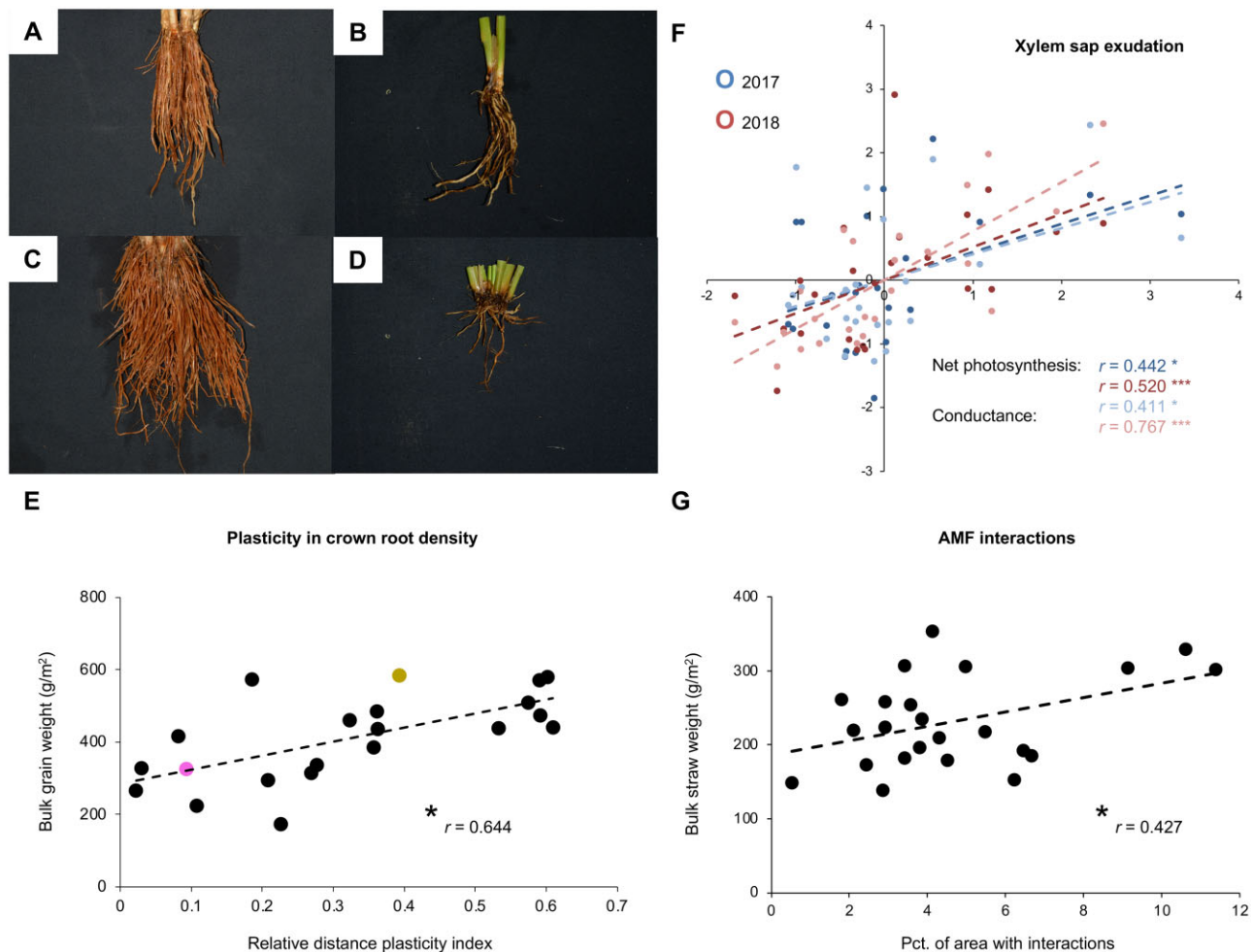


Figure 7 Gene expression patterns reflected links among root traits, leaf traits, and fitness. A, A crown root sample of the tropical japonica accession Azucena grown in wet conditions. B, A crown root sample of the same accession in dry conditions. C, Crown roots of the *circum*-aus accession Kasalath showed higher density in wet conditions than those of Azucena. D, However, crown root density of Kasalath showed higher levels of plasticity under drought and density was reduced to lower levels than Azucena. This response is likely to be independent of PSTOL1, since both accessions share the same haplotype at this locus. E, Pearson product-moment correlation between plasticity in crown root density and the fitness component bulk filled grain weight in the 2018 dry season ($P < 0.05$, $n = 21$). Azucena is indicated in pink and Kasalath in gold. F, Pearson correlation under drought between the physiological drought avoidance trait xylem sap exudation and net photosynthesis as well as stomatal conductance in the 2017 (blue) and 2018 (red) seasons ($P < 0.05$, $n = 24$). G, Pearson correlation between the intensity of rice root interactions with AM fungi and the fitness component bulk straw weight across wet and dry conditions ($P < 0.0374$, $n = 23$, shown) and within dry conditions (Pearson's $r = 0.853$, $P = 0.0008$, $n = 11$). Notation of significance for Pearson's r : $***P < 0.001$, $*P < 0.05$.

transcripts), the deepwater *circum*-aus accession Bhadoia 303 from Bangladesh was the most drought-responsive accession with 1,080 root DEGs. Strong plasticity in response to changing water availabilities has been observed for *circum*-aus accessions in previous instances, and it will be particularly interesting to see if these accessions could yield genetic variation that allows for successful plant responses to both drought and flooding (Xu et al., 2006; Hattori et al., 2009; Fukao et al., 2011; Kano et al., 2011; Bin Rahman and Zhang 2016; Sandhu et al., 2016).

This genetic and environmental variation in gene expression could be summarized in sets of root and shoot co-expression modules. Three of these modules were significantly tied to fitness and enriched in effects of signaling by

phytohormones (including auxin, ABA, and salicylic acid) known to mediate plant stress responses (Todaka et al., 2015; Gupta et al., 2020). The modules were further enriched in responses to the nutrient deprivation that comes with water limitation (Swift et al., 2019). Family members of the genes that constitute these modules, such as NAC domain TFs and phosphate transporters, appear to be involved in mediating drought-responsive changes in root growth, hydraulic conductivity, and nutrient loading into the xylem across plant species at least as distantly related to rice as the eudicot model plant *Arabidopsis thaliana* (Rosas et al., 2013; Tang et al., 2018).

The two fitness-associated root transcript modules were also enriched for aquaporin-encoding transcripts, which are

known to regulate water fluxes towards the shoot under drought stress (Henry et al., 2012; Grondin et al., 2016). In addition, the root modules were correlated with a cluster of co-expressed shoot transcripts enriched in biological processes related to photosynthesis. All three of the root and shoot co-expression modules were intimately linked with the hydraulic traits under selection, which involved xylem sap exudation, root osmotic potential and root density. Taken together, these data suggest positive fitness consequences of coordinated changes in an integrative set of molecular, physiological, and developmental traits.

In addition to finding evidence of ongoing selection on expression of the genes in these modules, we also uncovered signatures of past polygenic selection (Hämälä et al., 2020). The genomic regions underpinning the fitness-associated root and shoot transcript co-expression modules showed elevated genetic divergence (higher levels of F_{ST}) between temperate japonica accessions that are typically grown in stably wet irrigated environments, on the one hand, and indica as well as *circum*-aus accessions that are more often grown in drought-prone rainfed environments, on the other. The genomic regions further appeared subject to more frequent weak negative selection as evidenced by elevated levels of τ , based on a reference population consisting predominantly of rainfed-environment accessions (Gronau et al., 2013; Joly-Lopez et al., 2020). Similar patterns of weak negative or purifying selection have been observed previously in *A. thaliana* for a set of genes that are part of GO biological processes related to biotic interactions (Bakker et al., 2008), for which the fitness-linked co-expression modules we inferred were also enriched, including responses to bacteria, fungi, and insects, responses to chitin and salicylic acid, systemic acquired resistance, and biosynthesis of phenylpropanoids and fatty acids (Supplemental Data Sets S16 and S17).

Based on these signatures of ongoing and past selection on patterns of gene expression and on variation in physiological and developmental root and shoot traits that transcript levels were tied to, we hypothesized that traits inferred from the transcriptome data to be important for fitness could be validated in a different season. Indeed, a recent study on the rice leaf transcriptome showed that expression changes in response to environmental limitations in water and nutrient availability can have consistent associations with trait variation across seasons (Swift et al., 2019). In keeping with these expectations, the relevance of photosynthesis-related traits for plant fitness in wet and dry conditions that we inferred from our transcriptome data from the 2017 dry season was indeed visible in the subsequent dry season.

Importantly, our transcriptome data also identified fitness-linked traits from gene expression patterns in roots. Drought-induced expression changes that were tied to fitness under drought suggested that plants may respond adaptively to water limitation and concomitant P deficiency by intensifying interactions with AMF. Our hypothesis based

on these patterns and on previous studies of plant relations with AMF (Colard et al., 2011; Lanfranco et al., 2018; Mbodj et al., 2018; Yu et al., 2018), that interactions with AMF could have positive fitness consequences under drought, held up in the next dry season. We found that root interactions with AMF were positively linked with straw biomass, an important fitness component, within dry as well as between wet and dry field conditions. Future work will be necessary to establish the identities of the fungal interactions partners and to see how these interactions can be harnessed for rice resilience in breeding and agronomy programs (de Vries et al., 2020).

Our evolutionary systems biology approach allowed us to obtain unique insights into how a set of root and shoot traits across levels of biological organization integrates changes in both biotic and abiotic parameters upon drought and benefits rice fitness in lowland field conditions.

Materials and methods

Plant material

A core panel of 22 *O. sativa* accessions was selected from a panel of 215 landraces and breeding lines based on their phenotypic distributions for flowering time and leaf area in a 2016 dry-season field experiment at the International Rice Research Institute (IRRI) in Los Baños, Laguna, Philippines, which we described previously (Supplemental Figure S1 and Supplemental Data Set S1; Groen et al., 2020). The between-accession genetic distances were visualized using PCA (Kassambara, 2017) based on published DNA data for 179,634 single-nucleotide polymorphisms (Groen et al., 2020). The core included representatives from the *circum*-aus, indica, temperate japonica, (sub-)tropical japonica, and *circum*-basmati subgroups (Gutaker et al., 2020; Huang et al., 2012a; Wang et al., 2018). Seeds for all accessions were obtained from the International Rice Genebank Collection.

Establishment of field experiments

The first and main field experiment was conducted during the 2017 dry season at IRRI. Sixteen to twenty-four grams of seed from each accession was sown onto a seed bed on 1 December 2016, and at 18 days after sowing (DAS) seedlings were pulled and transplanted in a set of two experimental fields. The first one, designated UI (14°008'46.0"N 121°015'51.9"E), remained flooded as a wet paddy. The second field, located in a rain-out shelter (14°008'33.3"N 121°016'03.4"E) known as UR, remained flooded until irrigation was stopped and the field was drained to start the drought-stress treatment at 36 DAS.

The experiments were arranged in a randomized complete block design with each genotype planted in four replicates with one plant per hill in rectangular, 9 × 5-hill plots with 0.2 m × 0.25 m spacing for a total of 45 plants per plot. Basal fertilizer was applied at 33 DAS using complete fertilizer (14-14-14) of N₂, P₂O₅, and K₂O at the rate of 50 kg ha⁻¹ each. Manual weeding was conducted regularly in both fields.

Kuhol Buster and Actara were applied at 33 and 35 DAS, respectively, to control snail pests, while Actara was applied at 46 DAS and again at 61 and 69 DAS to control insect pests.

To monitor soil moisture levels in the dry field, soil water potential was recorded using two tensiometers (Soilmoisture Equipment) installed at a depth of 30 cm in each replicate. In addition, volumetric soil moisture was recorded at 10-cm depth increments, which was done by frequency domain reflectometry (Diviner 2000, Sentek) through 70-cm PVC tubes installed at nine locations throughout the field.

A second field experiment was set up in the 2018 dry season using the same protocol as much as possible (Supplemental Data Sets S20 and S21).

Shoot trait measurements

We measured a series of biochemical, physiological, morphological, and phenological traits in shoots to assess differences in drought response between genotypes and individuals. We measured Ψ_{leaf} at 49 and 50 DAS (early), and again at 69 and 70 DAS (late) in the wet and dry field, respectively. For this, we collected one leaf per replicate and stored it at -15°C . The leaves were pressed with a syringe after thawing and 10 μL of sap was pipetted onto a vapor pressure osmometer (Vapro model 5520, Wescor) to measure Ψ_{leaf} . We obtained shoot dry weights at 49 DAS (early), and again at 69 DAS (late) in both fields.

We measured plant height at 49, 55, and 63 DAS as early, intermediate and late time-points, respectively, and calculated the mean RGR using the formula $\text{mean RGR} = (\log_e H_{\text{final}} - \log_e H_{\text{initial}}) / t$, where t = time (days) between initial and final measurements of plant height (H; Hunt, 1982). We recorded flowering time as the day on which 50% of plants in a replicate plot flowered.

We selected six accessions as a mini-core for which we obtained additional measurements, including gene expression (see below). For the mini-core accessions we further measured chlorophyll fluorescence on a fully expanded leaf after illuminating at ambient light levels for 20 s using the pulse-amplitude-modulation technique (MINI-PAM, Walz, Effeltrich, Germany) at 50 DAS in both fields (early) and again at 63 and 64 DAS (late) in the wet and dry field, respectively. We calculated the efficiency of Photosystem II or quantum yield (Y_{II}) as $(F_m' - F_t) / F_m'$, where F_m' is the maximal fluorescence and F_t the steady-state terminal fluorescence (arbitrary units) (Genty et al., 1989). At 49 DAS (early), we counted tiller numbers and measured leaf areas in both fields. For the latter, we used a roller-belt-type leaf-area meter (Li-Cor, Model LI-3100C). The leaf-area data served as a basis to calculate the SLA through dividing by the leaf dry weight.

We further determined the stem-to-leaf ratio for plants in both fields at this time-point and collected a set of fully expanded leaves for assessing stomatal density. These leaves were first stored in 70% ethanol until we could take epidermal imprints from them at the midpoint of each leaf blade according to Kusumi (2013). For this, we used clear nail polish that we allowed to dry for 10–20 min before removing it

with cellophane tape. The imprints were transferred to a microscope slide and imaged at $10\times$ on a BX51 compound microscope fitted with a DP71 camera (Olympus). Images were processed and analyzed using ImageJ software version 1.52 (Abràmoff et al., 2004), and we counted the number of stomata in areas of $\sim 0.05 \text{ mm}^2$ between small veins under a magnification of $200\times$ (Wang et al., 2016; Cal et al., 2019).

We measured additional photosynthesis-related traits for the six mini-core accessions on which we focused our gene expression measurements. For these mini-core accessions we added leaf gas-exchange measurements with a portable LI-6400XT photosynthesis system (Li-Cor Biosciences). We made instantaneous measurements of CO_2 fixation (A) at a photosynthetic photon flux density of 1,000 (2017) or 1,500 (2018) $\mu\text{mol photons m}^{-2} \text{ s}^{-1}$ and a C_a of 400 $\mu\text{mol CO}_2 \text{ mol}^{-1}$, with the flow rate set to maintain a relative humidity of 65%, on one fully expanded leaf per replicate at 86 DAS (late) in the dry field. Before statistical analysis, the leaf gas-exchange data were filtered by excluding data points further than 3 standard deviations (SD) from the mean.

In the 2018 experiment, we measured the same set of biochemical, physiological, morphological, and phenological shoot traits that we measured for all 22 core accessions and the six mini-core accessions in the 2017 experiment. However, in this season we were able to measure the photosynthesis-related traits in both environments at 79 and 77 DAS (late) in the wet and dry fields, respectively.

Root trait measurements

We further measured a series of biochemical, physiological, and morphological traits in roots to assess differences in drought response between genotypes and individuals. We measured Ψ_{root} at 50 DAS (early) in both fields, and again at 69 and 70 DAS (late) in the wet and dry field, respectively. For this, we collected the crown roots of one plant per replicate, blotted them with dry tissue paper, then squeezed out excess water (from the well-watered paddy soil) using a syringe, and stored at -15°C inside the syringe until frozen. Samples were then thawed, the sap from the root tissue was pressed into a 2-mL tube using the syringe, and the resulting sap was centrifuged at 2,000g for 5 min to remove soil particles before pipetting 10 μL of sap onto a vapor pressure osmometer (Vapro model 5520, Wescor) to measure Ψ_{root} .

We measured the xylem sap exudation rate (both absolute and relative to shoot dry weight) at 49 and 50 DAS (early), and again at 69 and 70 DAS (late) in the wet and dry field, respectively, according to the protocol described by Morita and Abe (2002) and Henry et al. (2012). Starting at 07:00 h, shoots were cut at a height of around 15 cm from the soil surface. Sap emerging from the root zone was collected by covering the cut stems with a 625-cm² cotton towel inside a polyethylene bag that was sealed at the shoot base with a rubber band. After 4 h, the previously weighed towel, plastic bag, and rubber band were collected and reweighed immediately to quantify the sap exuded from the intact root system. Shoots were dried and weighed to

determine the biomass for each individual plant for each sampling date. One border row was left between individuals for each sampling date. All xylem sap exudation rate values were both analyzed as absolute measurements and as measurements normalized by the shoot mass of the individual from which sap was collected, to account for variation in plant size within and among genotypes.

Concurrent to the xylem sap exudation rate measurements, we sampled the sap exuded from the cut stems of adjacent plants to determine the sodium (Na^+) and potassium (K^+) ion content by pipetting sap droplets directly from the cut stems into a 2-mL micro-centrifuge tube. After diluting the samples ~ 100 -fold to obtain a volume of 10 mL, the samples were analyzed for ion concentration by atomic absorption spectrometry.

We analyzed the architecture of root crowns after excavating the root systems of one plant per replicate at 50 DAS (early) in both fields. Root crowns were excavated using a standard spade to a depth of 25 cm, and a radius of 25 cm around the shoot. We gently washed the root crowns in water before photographing them on a flat, black background accompanied by a scale marker. We then evaluated root traits using the online DIRT platform (Bucksch et al., 2014; Das et al., 2015), focusing on the crown root density.

In the 2018 experiment, we measured the same set of biochemical, physiological, and morphological root traits that we measured for all 22 core accessions in the 2017 experiment, plus the additional trait of interaction strength with arbuscular mycorrhizal fungi for the six mini-core accessions on which we focused our gene expression measurements in 2017. We assessed the interaction strength with arbuscular mycorrhizal fungi by performing chitin staining with trypan blue on root crown samples that were taken at 51 DAS (early). Per root system we imaged up to five patches of root area, with each patch $\sim 0.75 \text{ mm}^2$ in size, using a BX51 compound microscope fitted with a DP71 camera (Olympus). We inspected these rice root patches for infections by counting the number of intraradical fungal structures with a gridline intersect procedure (Paszkowski et al., 2006; Yang et al., 2012a). Before statistical analysis, the AM fungal count data were filtered by excluding data points further than 3 SD from the mean.

Trait plasticity was calculated as the RDPIs: $P_j = |Z_{j,k=2} - Z_{j,k=1}|/Z_{j,k=1}$, where j is genotype, k is the focal environment (1 = wet and 2 = dry), Z is the trait value, and P is the trait plasticity (Valladares et al., 2006).

Fitness or yield component characterization

At physiological maturity, all of the 7,920 plants that remained in the plots (i.e. individuals that had not undergone destructive sampling during the vegetative stage) were harvested and measured for yield component traits as proxies for plant fitness. These included crown root number as root trait, as well as stem width (cm), tiller number, plant height (cm), and panicle length (cm) as shoot traits. Filled and unfilled grains were sorted and separated from the straw and their bulk dry weights per 1 m^2 were obtained

after drying to 14% moisture content in an oven at 45°C for three days. The bulked weights of filled grains, unfilled grains, and straw were then used to calculate the harvest index as the ratio of filled grain dry weight to the total shoot dry weight (filled and unfilled grain plus straw).

Quantitative genetic analysis

Trait measures were processed using analysis of variance (ANOVA) to partition phenotypic variation. Using the lme4 package version 1.1 in R (Bates et al., 2015; R Core Team, 2020), we fit mixed-effect general linear models for every trait, which included terms for accession or genotype (G) as random factor, field environment (E) as fixed factor, interaction between them ($G \times E$) as random factor and error variance (ϵ). Significance for each factor was tested using an F test and judged using two-tailed P -values. We estimated broad-sense heritability for each trait as $H^2 = 0.5 \times \sigma_G^2 / (0.5 \times \sigma_G^2 + (0.5 \times \sigma_{GE}^2/e) + (\sigma_E^2/re))$, with σ_G^2 , σ_{GE}^2 and σ_E^2 as the among-genotype, $G \times E$ and within-genotype variance components, e as the number of environments and r as the replicate number per environment. Because *O. sativa* is predominantly selfing, we adjusted for the twofold overestimation of additive genetic variance among inbred accessions by applying the factor 0.5 (Keurentjes et al., 2007).

Tissue collection for RNA-Seq

Leaf blade and crown root tip sampling was performed in 2017 at 50 DAS (early) on replicate plants over four plots for each of the six mini-core accessions in the wet and dry field from 10:00 h to 12:00 h (4 h after dawn) as described previously (Groen et al., 2020). Four pairs of technicians collected leaf and root tissue in each field, and both fields were sampled simultaneously in the same order by replicate and plot by different teams.

For leaves, two fully expanded leaf blades were selected for sampling. Approximately 12 cm of leaf length was cut into small pieces and submerged into 4-mL chilled RNALater solution in 5-mL screw-cap tubes. For roots, root systems of one plant per replicate in the wet field and four plants per replicate in the dry field were excavated gently using a standard spade. Newly emerging, intact nodal root tips were cut at the base using scissors and submerged into 4-mL chilled RNALater solution in 5-mL screw-cap tubes.

Scissors used for tissue sampling were wiped with 70% ethanol between each plot to avoid contamination. The 96 5-mL tubes with individual tissue samples were placed on ice in styrofoam ice chests, then transferred to a cold room at 4°C overnight. Samples from each of the tubes were then transferred into pairs of 2-mL tubes before being stored at -80°C . Each tube was sent to New York University's Center for Genomics and Systems Biology on dry ice to be processed further for mRNA sequencing and long-term storage.

RNA extraction, library preparation, and sequencing

Frozen leaf-blade and root samples were thawed at room temperature and blotted briefly on a KimWipe to remove excess RNALater. The bulk tissue was then flash-frozen in

liquid nitrogen and pulverized with pre-cooled mortar and pestle (CoorsTek) to allow extraction of total RNA with the RNeasy Plant Mini Kit according to manufacturer's protocol (QIAGEN). The RNA was quantified on a Qubit (Invitrogen) before assessing RNA quality on an Agilent BioAnalyzer (Agilent Technologies). The total RNA preps were then stored in nuclease-free water at -80°C .

Total RNA was processed for each individual sample according to a barcoded plate-based 3' mRNA-seq protocol, as described previously (Groen et al., 2020). This modified version of the switch mechanism at the 5' end of RNA templates (SMART)-seq2 and single cell RNA barcoding and sequencing (SCRB)-seq protocols allowed multiplexed pooling of 96 samples before library preparation with the Nextera XT DNA sample prep kit (Illumina). The protocol returned 3'-biased cDNA fragments similar to the Drop-Seq protocol (Macosko et al., 2015). The library consisted of 96 pooled sister samples, i.e. 24 leaf and 24 root samples from the wet field were matched with plant samples from the same tissues and plot numbers in the dry field. We quantified the cDNA library on an Agilent BioAnalyzer and sequenced it on the Illumina NextSeq 500 in the 2×50 -base mode using the following settings: read 1 was 20 bp (bases 1–12 sample barcode, bases 13–20 unique molecular identifier [UMI]), and read 2 (paired end) was 50 bp.

RNA-Seq data processing

The 3'-mRNA-seq reads were quantified as described by Groen et al. (2020) according to the Drop-Seq Cookbook from the McCarroll lab using Drop-seq tools v1.12 (J Nemesh, A Wysoker, <https://www.github.com/broadinstitute/Drop-seq/releases>): a wrapper for aligning and parsing not only the reads, but also their embedded barcodes, with STAR aligner v020201. STAR used the Nipponbare IRGSP 1.0 (GCF_001433935.1) genome, including plastids, as reference. A reference annotation was generated from Ensembl's IRGSP nuclear *O. sativa* genome annotation v1.0.37 (ftp://ftp.ensemblgenomes.org/pub/plants/release-37/gff3/oryza_sativa) and supplemented with Refseq's Mitochondrial and Chloroplast annotations (ftp://ftp.ncbi.nlm.nih.gov/genomes/all/GCF/001/433/935/GCF_001433935.1_IRGSP-1.0). Metadata were generated with Drop-Seq and Picard tools (<https://www.broadinstitute.github.io/picard/>). The genome and annotations were indexed using STAR (genomeGenerate with options `-runThreadN 12 -genomeDir inc_plastids -genomeFastaFiles Oryza_sat_CpMt.fa -sjdbGTFfile 1.0.37_all.gtf -sjdbOverhang 49`). Where applicable, annotations were converted between RAP-DB and MSU-7 IDs using the conversion table from the Rice Annotation Project (RAP-MSU_2017-04-14.txt, the latest version can be found at <https://rapdb.dna.affrc.go.jp/download/irgsp1.html>). For quantification, raw reads were first converted from fastq to unaligned bam format using Picard tools' FastqToSam and subsequently processed using the unified script (Drop-seq_alignment.sh) in what is essentially default mode for a fastq starting format. Digital gene expression (DGE) profiles were then generated with the

DigitalExpression utility using an expected number of barcodes of 96. For QA purposes the DGE profiles were output both as UMI count and raw read count matrices with samples as columns and transcripts as rows. The values analyzed represent the number of UMIs that were detected.

To account for differences in the total read number per sample, we normalized UMI counts from each sample by dividing by the total number of UMIs detected in that sample. These numbers were multiplied by 1×10^6 for conversion to transcripts-per-million. This scaling factor largely represents a consistent increase or decrease across all positive counts in our data matrix. After this, the normalized read counts were subject to blind variance stabilizing transformation provided by the DESeq2 package (Love et al., 2014; R Core Team, 2020).

Differential expression

Prior to differential expression analysis the data matrix was split between leaf and root samples. For each organ type, samples were analyzed for DEGs using the DESeq2 package to test for differential transcript expression between each pair of accessions within and among the wet and dry environments using the model: $\text{Expression} \sim \text{Genotype} + \text{Environment} + \text{Genotype} \times \text{Environment}$. To detect DEGs, a 5% false discovery rate (FDR) correction for multiple comparisons was determined (Storey and Tibshirani, 2003), and a minimal $|1.0| \log_2$ fold change threshold was applied. Contrasts were also generated between the wet and dry environments overall. Despite the lenient threshold for minimum fold change, only a few DEGs were detected for leaf-expressed genes between the environments overall, and contrasts between pairs of accessions were only analyzed further for root transcriptomes. For the root samples, private versus common drought-responsive DEGs between accessions were analyzed using Upset diagrams created with the publicly available software Intervene (<https://asntech.shinyapps.io/intervene>). PCA was performed to explore the gene expression profiles and visualize between-sample distances (Kassambara, 2017).

Gene co-expression analysis

The variance-stabilized gene expression matrices for leaves and roots were used for the construction of gene co-expression networks using the WGCNA package (Langfelder and Horvath, 2008), with the soft power parameter (β) set to 6 to ensure that the resulting network exhibited an approximately scale-free topology, the *P*-value ratio threshold for reassigning transcripts between modules set to 0, the cut height of the dendrogram to merge modules set to 0.25, and the minimum size of modules set to 10 transcripts.

Gene set enrichment analysis

We performed gene set enrichment analysis to gather further biological insight into the DEGs and transcript modules. We considered GO biological processes, using PANTHER's Overrepresentation Test (released February 24, 2021) with the *O. sativa* genes in the GO database (DOI: 10.5281/

zenodo.4495804; released February 1, 2021) as background gene set used to match the foreground set (Mi et al., 2021), as well as TF binding motifs within 300 bp of the transcription start site, using ShinyGO v0.61 (Ge et al., 2020). Enrichment was calculated using Fisher's exact tests followed by FDR correction on two-tailed P -values. For root co-expression module 11, we added an analysis for enrichment of TF binding motifs to regions within 600 bp of the transcription start site to increase the number of results. For analyses of enrichment in root modules 1 and 11 of genes targeted by PSTOL1 and for genes responsive to interactions with AM fungi we compared our data to sets of genes that were differentially expressed in *Pro35S:PSTOL1*_{Kasalath} transgenic IR64 plants compared to IR64 plants (Gamuyao et al., 2012), and differentially expressed upon crown-root colonization by AM fungi (Gutjahr et al., 2015), respectively. Transcript annotations were converted between RAP-DB and MSU-7 IDs using RAP's conversion table to make these two datasets compatible with ours (RAP-MSU_2017-04-14.txt, the latest version is available at <https://rapdb.dna.affrc.go.jp/download/irgsp1.html>).

Associations between transcript modules, functional traits, and fitness

Before we could identify associations between transcript modules, functional traits, and fitness for the rice populations across the field environments, we first calculated an "eigengene" for each transcript co-expression module. The eigengene is the first principal component of a module and represents the expression trends of all transcripts that are members of a particular module (Langfelder and Horvath, 2008). The eigengene of each module as well as the standardized trait values for each functional trait and fitness component were then combined into a matrix and Pearson product-moment correlations were computed between each module eigengene on the one hand, and the functional-trait and fitness data on the other, using regression models: $Y = \mu + T + \varepsilon$, where Y represents the functional trait or fitness component of interest, μ an intercept parameter, T denotes the transcript module covariate, and ε residual error. Associations with fitness components and traits were deemed significant when they exhibited Bonferroni-adjusted, two-tailed P -values of $P < 3.46 \times 10^{-4}$ for shoots and $P < 2.50 \times 10^{-4}$ for roots, respectively (Bland and Altman, 1995). Path analysis was performed with the package lavaan version 0.6.6 (Rosseel, 2012), which was implemented in R version 4.0.1 (R Core Team, 2020).

Pairwise population divergence statistics for transcript modules

The pairwise population divergence statistics (F_{ST}) had been computed as described (Nordborg et al., 2005), using a 100-kb window, between temperate japonica landraces on the one hand, and either *circum-aus*, *indica*, or tropical japonica landraces on the other, respectively (Huang et al., 2010).

Values were downloaded from a follow-up study (Huang et al., 2012b).

Variation in F_{ST} across the genome for these subgroups is of interest in that windows with very high or low values may be seen as candidates for harboring selectively important loci (Lewontin and Krakauer, 1973; Akey et al., 2002; Hämmälä et al., 2020), as previously demonstrated for identifying genome regions linked to salinity tolerance in African rice, *Oryza glaberrima* (Meyer et al., 2016).

Each transcript was assigned the F_{ST} value from the genomic region (as a 100-kb window) in which its coding gene was located. We then combined the co-expression module assignments for each transcript with the estimates of sequence evolution to analyze whether selection may be acting differently on the collection of genomic regions giving rise to transcripts that are part of fitness-linked co-expression modules in root and shoot tissue. Estimates of genetic divergence between subgroups for this collection of genomic regions were acquired by averaging the F_{ST} estimates of the individual regions. These were compared against average F_{ST} estimates from genomic regions harboring root- and/or shoot-expressed genes elsewhere in the genome using Welch's t test to account for unequal variances and sample sizes between groups (Welch, 1947).

To find additional evidence of selection on the collection of genomic regions linked to fitness by virtue of giving rise to transcripts that made up shoot module 8 and root modules 1 and 11, we also considered the fraction of sites under any kind of selection ρ and the fraction of polymorphisms under weak negative selection τ of these regions using GreenINSIGHT (Gronau et al., 2013; Joly-Lopez et al., 2020), and compared these to fractions of sites under selection in other genomic regions using the same approach we used for F_{ST} . Data were visualized using PlotsOfData (Postma and Goedhart, 2019).

Accession numbers

Raw RNA sequence data have been deposited as part of SRA BioProject PRJNA564338. Processed RNA expression counts, alongside a key to the RNA sequence data in SRA BioProject PRJNA564338 and the sample metadata, have been deposited in Zenodo under DOI 10.5281/zenodo.4779049. VST-normalized count data can be found in the supplemental material.

Supplemental data

The following materials are available in the online version of this article.

Supplemental Figure S1. Overview of the core panel of rice accessions selected for this study.

Supplemental Figure S2. Description of the wet and dry field environments during the 2017 dry season.

Supplemental Figure S3. Root and shoot samples of the mini-core panel accessions could be separated based on their genome-wide gene expression profiles.

Supplemental Figure S4. Accession-specific changes to root gene expression in dry versus wet conditions.

Supplemental Figure S5. A flowchart of the analysis correlating transcript co-expression modules with functional traits and fitness.

Supplemental Figure S6. Two fitness-linked root co-expression modules integrate responses to changing abiotic and biotic factors under drought and are regulated by drought-responsive TFs.

Supplemental Figure S7. Rainfall and vapor-pressure deficit differed between the 2017 and 2018 dry seasons.

Supplemental Data Set S1. List of accessions of the core and mini-core diversity panels.

Supplemental Data Set S2. Experiment timeline, and data on trait as well as fitness component measurements for the 2017 dry season.

Supplemental Data Set S3. Data on weather and soil characteristics during the 2017 dry season.

Supplemental Data Set S4. Genetic correlations between absolute trait values under drought, trait plasticity values under drought and plant fitness.

Supplemental Data Set S5. Overview of library preparation and transcriptome sequencing for roots and shoots of mini-core accessions.

Supplemental Data Set S6. Normalized transcript level counts for shoots of mini-core accessions.

Supplemental Data Set S7. Normalized transcript level counts for roots of mini-core accessions.

Supplemental Data Set S8. Principal component analyses of RNA-seq samples separated per tissue type and combined.

Supplemental Data Set S9. DEGs in rice shoots and enriched GO biological processes among them.

Supplemental Data Set S10. DEGs in rice roots.

Supplemental Data Set S11. Overlap between accessions in DEGs in roots and enriched GO biological processes among overlapping genes.

Supplemental Data Set S12. Root and shoot modules of co-expressed transcripts.

Supplemental Data Set S13. Correlations among traits, fitness, and shoot gene co-expression module eigengenes.

Supplemental Data Set S14. Correlations among traits, fitness, and root gene co-expression module eigengenes.

Supplemental Data Set S15. Effects of genotype and environment on expression variation in transcript co-expression modules.

Supplemental Data Set S16. Gene set enrichment analysis of fitness-linked shoot co-expression module 8.

Supplemental Data Set S17. Gene set enrichment analysis of fitness-linked root co-expression modules 1 and 11.

Supplemental Data Set S18. Expression of marker genes for root interactions with arbuscular mycorrhizal fungi.

Supplemental Data Set S19. Analyses of polygenic selection on fitness-linked root and shoot co-expression modules.

Supplemental Data Set S20. Experiment timeline, and data on trait as well as fitness component measurements for the 2018 dry season.

Supplemental Data Set S21. Comparison of weather and soil characteristics between the 2017 and 2018 dry seasons.

Supplemental Data Set S22. Repeatability of traits between seasons, and correlations between root density and plant fitness components in the 2018 dry season.

Supplemental Data Set S23. Correlations between shoot traits and fitness components in the 2018 dry season.

Supplemental Data Set S24. Correlations between levels of root interactions with arbuscular mycorrhizal fungi and fitness components in the 2018 dry season.

Acknowledgments

We thank Leonardo Holongbayan, Eleanor Mico, Nancy Sadiasa, Lesly Satioquia, Bianca Uzziel Principe, and Philip Zamborano for assistance with trait measurements, tissue sampling and field management, IRRI's Climate Unit staff for providing weather data, the NYU Center for Genomics and Systems Biology GenCore Facility for sequencing support, and NYU High Performance Computing for supplying computational resources. We are grateful to Bruno Guillotin, Ken Birnbaum, Veronica Roman-Reyna, Ricardo Oliva, as well as members of the Purugganan laboratory and IRRI's Strategic Innovation and Rice Breeding research platforms for insightful discussions.

Funding

This work was funded in part by grants from the Zegar Family Foundation, the National Science Foundation Plant Genome Research Program and NYU Abu Dhabi Research Institute to M.D.P., a fellowship from the Gordon and Betty Moore Foundation/Life Sciences Research Foundation (Grant GBMF2550.06) and University of California at Riverside startup funds to S.C.G., and a fellowship from the Natural Sciences and Engineering Research Council of Canada to Z.J.-L. (Grant PDF-502464-2017).

Conflict of interest statement. None declared.

References

- Abràmoff MD, Magalhães, PJ, Ram SJ** (2004) Image processing with ImageJ. *Biophotonics Int* **11**: 36–42.
- Akey JM, Zhang G, Zhang K, Jin L, Shriver MD** (2002) Interrogating a high-density SNP map for signatures of natural selection. *Genome Res* **12**: 1805–1812
- Bakker EG, Traw MB, Toomajian C, Kreitman M, Bergelson J** (2008) Low levels of polymorphism in genes that control the activation of defense response in *Arabidopsis thaliana*. *Genetics* **178**: 2031–2043
- Bates D, Maechler M, Bolker B, Walker S** (2015) Fitting linear mixed-effects models using lme4. *J Stat Softw* **67**: 1–48
- Bin Rahman AR, Zhang J** (2016) Flood and drought tolerance in rice: opposite but may coexist. *Food Energy Secur* **5**: 76–88

- Bland JM, Altman DG** (1995) Multiple significance tests: the Bonferroni method. *BMJ* **310**: 170
- Bucksch A, Burr ridge J, York LM, Das A, Nord E, Weitz JS, Lynch JP** (2014) Image-based high-throughput field phenotyping of crop roots. *Plant Physiol* **166**: 470–486
- Cal AJ, Sanciangco M, Rebolledo MC, Luquet D, Torres RO, McNally KL, Henry A** (2019) Leaf morphology, rather than plant water status, underlies genetic variation of rice leaf rolling under drought. *Plant Cell Environ* **42**: 1532–1544
- Calvin M** (1956) The photosynthetic cycle. *Bull Soc Chim Biol* **38**: 1233–1244
- Campbell-Staton SC, Winchell KM, Rochette NC, Fredette J, Maayan I, Schweizer RM, Catchen J** (2020) Parallel selection on thermal physiology facilitates repeated adaptation of city lizards to urban heat islands. *Nat Ecol Evol* **4**: 652–658
- Catolos M, Sandhu N, Dixit S, Shamsudin NA, Naredo ME, McNally KL, Henry A, Diaz MG, Kumar A** (2017) Genetic loci governing grain yield and root development under variable rice cultivation conditions. *Front Plant Sci* **8**: 1763
- Chen H, Jiang JG** (2010) Osmotic adjustment and plant adaptation to environmental changes related to drought and salinity. *Environ Rev* **18**: 309–319
- Chin JH, Gamuyao R, Dalid C, Bustamam M, Prasetyono J, Moeljopawiro S, Wissuwa M, Heuer S** (2011) Developing rice with high yield under phosphorus deficiency: *Pup1* sequence to application. *Plant Physiol* **156**: 1202–1216
- Colard A, Angelard C, Sanders IR** (2011) Genetic exchange in an arbuscular mycorrhizal fungus results in increased rice growth and altered mycorrhiza-specific gene transcription. *Appl Environ Microbiol* **77**: 6510–6515
- Das A, Schneider H, Burr ridge J, Ascanio AKM, Wojciechowski T, Topp CN, Lynch JP, Weitz JS, Bucksch A** (2015) Digital imaging of root traits (DIRT): a high-throughput computing and collaboration platform for field-based root phenomics. *Plant Methods* **11**: 51
- Des Marais DL, McKay JK, Richards JH, Sen S, Wayne T, Juenger TE** (2012) Physiological genomics of response to soil drying in diverse *Arabidopsis* accessions. *Plant Cell* **24**: 893–914
- Dixit S, Grondin A, Lee CR, Henry A, Mitchell-Olds, T, Kumar A** (2015) Understanding rice adaptation to varying agro-ecosystems: trait interactions and quantitative trait loci. *BMC Genet* **16**: 86
- Dwivedi JL, HilleRisLambers D, Senadhira D** (1992) Rapid and non-destructive screening technique for elongation in deepwater rice (DWR) using gibberellic acid (GA₃). *Int Rice Res Notes* **17**: 13–14
- Fiorilli V, Vallino M, Biselli C, Faccio A, Bagnaresi P, Bonfante P** (2015) Host and non-host roots in rice: cellular and molecular approaches reveal differential responses to arbuscular mycorrhizal fungi. *Front Plant Sci* **6**: 636
- Fukao T, Yeung E, Bailey-Serres J** (2011) The submergence tolerance regulator SUB1A mediates crosstalk between submergence and drought tolerance in rice. *Plant Cell* **23**: 412–427
- Gamuyao R, Chin JH, Pariasca-Tanaka J, Pesaresi P, Catausan S, Dalid C, Slamet-Loedin I, Tecson-Mendoza EM, Wissuwa M, Heuer S** (2012) The protein kinase Pstol1 from traditional rice confers tolerance of phosphorus deficiency. *Nature* **488**: 535–539
- Ge SX, Jung D, Yao R** (2020) ShinyGO: a graphical gene-set enrichment tool for animals and plants. *Bioinformatics* **36**: 2628–2629
- Genty B, Briantais JM, Baker NR** (1989) The relationship between the quantum yield of photosynthetic electron transport and quenching of chlorophyll fluorescence. *Biochim Biophys Acta Gen Subj* **990**: 87–92
- Gerke J** (1995) Chemische Prozesse der Nährstoffmobilisierung in der Rhizosphäre und ihre Bedeutung für den Übergang vom Boden in die Pflanze. Cuvillier
- Groen SC** (2016) Signalling in systemic plant defence—roots put in hard graft. *J Exp Bot* **67**: 5585–5587
- Groen SC, Purugganan MD** (2016) Systems genetics of plant adaptation to environmental stresses. *Am J Bot* **103**: 1–3
- Groen SC, Calic I, Joly-Lopez Z, Platts AE, Choi JY, Natividad M, Dorph K, Mauck WM, Bracken B, Cabral CLU, et al.** (2020) The strength and pattern of natural selection on gene expression in rice. *Nature* **578**: 572–576
- Gronau I, Arbiza L, Mohammed J, Siepel A** (2013) Inference of natural selection from interspersed genomic elements based on polymorphism and divergence. *Mol Biol Evol* **30**: 1159–1171
- Grondin A, Dixit S, Torres RO, Venkateshwarlu C, Rogers E, Mitchell-Olds T, Benfey PN, Kumar A, Henry A** (2018) Physiological mechanisms contributing to the QTL *qDTY3.2* effects on improved performance of rice Moroberekan × Swarna BC₂F_{3:4} lines under drought. *Rice* **11**: 43
- Grondin A, Mauleon R, Vadez V, Henry A** (2016) Root aquaporins contribute to whole plant water fluxes under drought stress in rice (*Oryza sativa* L.). *Plant Cell Environ* **39**: 347–365
- Güimil S, Chang HS, Zhu T, Sesma A, Osbourn A, Roux C, Ioannidis V, Oakeley EJ, Docquier M, Descombes P, et al.** (2005) Comparative transcriptomics of rice reveals an ancient pattern of response to microbial colonization. *Proc Natl Acad Sci USA* **102**: 8066–8070
- Gupta A, Rico-Medina A, Caño-Delgado AI** (2020) The physiology of plant responses to drought. *Science* **368**: 266–269
- Gutaker RM, Groen SC, Bellis ES, Choi JY, Pires IS, Bocinsky RK, Slayton ER, Wilkins O, Castillo CC, Negrão S, et al.** (2020) Genomic history and ecology of the geographic spread of rice. *Nat Plants* **6**: 492–502
- Gutjahr C, Banba M, Croset V, An K, Miyao A, An G, Hirochika H, Imaizumi-Anraku H, Paszkowski U** (2008) Arbuscular mycorrhiza-specific signaling in rice transcends the common symbiosis signaling pathway. *Plant Cell* **20**: 2989–3005
- Gutjahr C, Casieri L, Paszkowski U** (2009) *Glomus intraradices* induces changes in root system architecture of rice independently of common symbiosis signaling. *New Phytol* **182**: 829–837
- Gutjahr C, Paszkowski U** (2009) Weights in the balance: jasmonic acid and salicylic acid signaling in root-biotroph interactions. *Mol Plant-Microbe Interact* **22**: 763–772
- Gutjahr C, Radovanovic D, Geoffroy J, Zhang Q, Siegler H, Chiapello M, Casieri L, An K, An G, Guiderdoni E, et al.** (2012) The half-size ABC transporters STR1 and STR2 are indispensable for mycorrhizal arbuscule formation in rice. *Plant J* **69**: 906–920
- Gutjahr C, Sawers RJ, Marti G, Andrés-Hernández L, Yang SY, Casieri L, Angliker H, Oakeley EJ, Wolfender JL, Abreu-Goodger C, et al.** (2015) Transcriptome diversity among rice root types during asymbiosis and interaction with arbuscular mycorrhizal fungi. *Proc Natl Acad Sci USA* **112**: 6754–6759
- Hämälä T, Guiltinan MJ, Marden JH, Maximova SN, dePamphilis CW, Tiffin P** (2020) Gene expression modularity reveals footprints of polygenic adaptation in *Theobroma cacao*. *Mol Biol Evol* **37**: 110–123
- Hattori Y, Nagai K, Furukawa S, Song XJ, Kawano R, Sakakibara H, Wu J, Matsumoto T, Yoshimura A, Kitano H, et al.** (2009) The ethylene response factors SNORKEL1 and SNORKEL2 allow rice to adapt to deep water. *Nature* **460**: 1026–1030
- Henry A, Cal AJ, Batoto TC, Torres RO, Serraj R** (2012) Root attributes affecting water uptake of rice (*Oryza sativa*) under drought. *J Exp Bot* **63**: 4751–4763
- Henry A, Gowda VR, Torres RO, McNally KL, Serraj R** (2011) Variation in root system architecture and drought response in rice (*Oryza sativa*): phenotyping of the OryzaSNP panel in rainfed lowland fields. *Field Crops Res* **120**: 205–214
- Henry A, Wehler R, Grondin A, Franke R, Quintana M** (2016) Environmental and physiological effects on grouping of drought-tolerant and susceptible rice varieties related to rice (*Oryza sativa*) root hydraulics under drought. *Ann Bot* **118**: 711–724
- Hossain MA, Lee Y, Cho JI, Ahn CH, Lee SK, Jeon JS, Kang H, Lee CH, An G, Park PB** (2010) The bZIP transcription factor OsABF1

- is an ABA responsive element binding factor that enhances abiotic stress signaling in rice. *Plant Mol Biol* **72**: 557–566
- Hou FY, Huang J, Yu SL, Zhang HS** (2007) The 6-phosphogluconate dehydrogenase genes are responsive to abiotic stresses in rice. *J Integr Plant Biol* **49**: 655–663
- Huang X, Sang T, Zhao Q, Feng Q, Zhao Y, Li C, Zhu C, Lu T, Zhang Z, Li M, et al.** (2010) Genome-wide association studies of 14 agronomic traits in rice landraces. *Nat Genet* **42**: 961–967
- Huang X, Kurata N, Wang ZX, Wang A, Zhao Q, Zhao Y, Liu K, Lu H, Li W, Guo Y, et al.** (2012a) A map of rice genome variation reveals the origin of cultivated rice. *Nature* **490**: 497–501.
- Huang X, Zhao Y, Li C, Wang A, Zhao Q, Li W, Guo Y, Deng L, Zhu C, Fan D, et al.** (2012b) Genome-wide association study of flowering time and grain yield traits in a worldwide collection of rice germplasm. *Nat Genet* **44**: 32–39.
- Hunt R** (1982) *Plant Growth Curves: The Functional Approach to Plant Growth Analysis*. Edward Arnold, London
- Jeong K, Mattes N, Catausan S, Chin JH, Paszkowski U, Heuer S** (2015) Genetic diversity for mycorrhizal symbiosis and phosphate transporters in rice. *J Integr Plant Biol* **57**: 969–979
- Joly-Lopez Z, Platts AE, Gulko B, Choi JY, Groen SC, Zhong X, Siepel A, Purugganan, MD** (2020) An inferred fitness consequence map of the rice genome. *Nat Plants* **6**: 119–130
- Kano M, Inukai Y, Kitano H, Yamauchi A** (2011) Root plasticity as the key root trait for adaptation to various intensities of drought stress in rice. *Plant Soil* **342**: 117–128
- Kassambara A** (2017) Practical guide to principal component methods in R: PCA, M (CA), FAMD, MFA, HCPC, factextra. *STHDA*
- Kawakatsu T, Teramoto S, Takayasu S, Maruyama N, Nishijima R, Kitomi Y, Uga Y** (2021) The transcriptomic landscapes of rice cultivars with diverse root system architectures grown in upland field conditions. *Plant J* **106**: 1177–1190
- Keurentjes JJB, Fu J, Terpstra IR, Garcia JM, van den Ackerveken G, Snoek LB, Peeters AJM, Vreugdenhil D, Koornneef M, Jansen RC** (2007) Regulatory network construction in *Arabidopsis* by using genome-wide gene expression quantitative trait loci. *Proc Natl Acad Sci USA* **104**: 1708–1713
- Kleessen S, Laitinen R, Fusari CM, Antonio C, Sulpice R, Fernie AR, Stitt M, Nikoloski Z** (2014) Metabolic efficiency underpins performance trade-offs in growth of *Arabidopsis thaliana*. *Nat Commun* **5**: 3537
- Kobayashi T, Ozu A, Kobayashi S, An G, Jeon JS, Nishizawa NK** (2019) OsbHLH058 and OsbHLH059 transcription factors positively regulate iron deficiency responses in rice. *Plant Mol Biol* **101**: 471–486
- Kondo M, Aguilar A, Abe J, Morita S** (2000) Anatomy of nodal roots in tropical upland and lowland rice varieties. *Plant Prod Sci* **3**: 437–445
- Kumar A, Dixit S, Ram T, Yadaw RB, Mishra KK, Mandal NP** (2014) Breeding high-yielding drought-tolerant rice: genetic variations and conventional and molecular approaches. *J Exp Bot* **65**: 6265–6278
- Kusumi K** (2013) Measuring stomatal density in rice. *Bio Prot* **3**: e753
- Lanfranco L, Fiorilli V, Gutjahr C** (2018) Partner communication and role of nutrients in the arbuscular mycorrhizal symbiosis. *New Phytol* **220**: 1031–1046
- Langfelder P, Horvath S** (2008) WGCNA: an R package for weighted correlation network analysis. *BMC Bioinformatics* **9**: 559
- Lee DK, Chung PJ, Jeong JS, Jang G, Bang SW, Jung H, Kim YS, Ha SH, Choi YD, Kim JK** (2017) The rice OsNAC6 transcription factor orchestrates multiple molecular mechanisms involving root structural adaptations and nicotianamine biosynthesis for drought tolerance. *Plant Biotech J* **15**: 754–764
- Levitt J** (1980) *Responses of Plants to Environmental Stresses: Water, Radiation, Salt, and Other Stresses*. Vol II, Academic Press, Cambridge, MA
- Lewontin RC, Krakauer J** (1973) Distribution of gene frequency as a test of the theory of the selective neutrality of polymorphisms. *Genetics* **74**: 175–195
- Li Q, Chen L, Yang A** (2020) The molecular mechanisms underlying iron deficiency responses in rice. *Int J Mol Sci* **21**: 43
- Love MI, Huber W, Anders S** (2014) Moderated estimation of fold change and dispersion for RNA-seq data with DESeq2. *Genome Biol* **15**: 550
- Macosko EZ, Basu A, Satija R, Nemesh J, Shekhar K, Goldman M, Tirosh I, Bialas AR, Kamitaki N, Martersteck EM, et al.** (2015) Highly parallel genome-wide expression profiling of individual cells using nanoliter droplets. *Cell* **161**: 1202–1214
- Mao C, He J, Liu L, Deng Q, Yao X, Liu C, Qiao Y, Li P, Ming F** (2020) OsNAC2 integrates auxin and cytokinin pathways to modulate rice root development. *Plant Biotech J* **18**: 429–442
- Mbodj D, Effa-Effa B, Kane A, Manneh B, Gantet P, Laplaze L, Diedhiou AG, Grondin A** (2018) Arbuscular mycorrhizal symbiosis in rice: establishment, environmental control and impact on plant growth and resistance to abiotic stresses. *Rhizosphere* **8**: 12–26
- Meyer RS, Choi JY, Sanches M, Plessis A, Flowers JM, Amas J, Dorph K, Barretto A, Gross B, Fuller DQ, et al.** (2016) Domestication history and geographical adaptation inferred from a SNP map of African rice. *Nat Genet* **48**: 1083–1088
- Mi H, Ebert D, Muruganujan A, Mills C, Albou LP, Mushayamaha T, Thomas PD** (2021) PANTHER version 16: a revised family classification, tree-based classification tool, enhancer regions and extensive API. *Nucleic Acids Res* **49**: D394–D403
- Miao C, Xiao L, Hua K, Zou C, Zhao Y, Bressan RA, Zhu JK** (2018) Mutations in a subfamily of abscisic acid receptor genes promote rice growth and productivity. *Proc Natl Acad Sci USA* **115**: 6058–6063
- Morita S, Abe J** (2002) Diurnal and phenological changes of bleeding rate in lowland rice plants. *Jpn J Crop Sci* **71**: 383–388
- Mukhopadhyay P, Tyagi AK** (2015) OsTCP19 influences developmental and abiotic stress signaling by modulating ABI4-mediated pathways. *Sci Rep* **5**: 9998
- Nagano AJ, Sato Y, Mihara M, Antonio BA, Motoyama R, Itoh H, Nagamura Y, Izawa T** (2012) Deciphering and prediction of transcriptome dynamics under fluctuating field conditions. *Cell* **151**: 1358–1369
- Nicotra AB, Atkin OK, Bonser SP, Davidson AM, Finnegan EJ, Mathesius U, Poot P, Purugganan MD, Richards CL, Valladares F, et al.** (2010) Plant phenotypic plasticity in a changing climate. *Trends Plant Sci* **15**: 684–692
- Nordborg M, Hu TT, Ishino Y, Jhaveri J, Toomajian C, Zheng H, Bakker E, Calabrese P, Gladstone J, Goyal R, et al.** (2005) The pattern of polymorphism in *Arabidopsis thaliana*. *PLoS Biol* **3**: e196
- Nguyen MX, Moon S, Jung KH** (2013) Genome-wide expression analysis of rice aquaporin genes and development of a functional gene network mediated by aquaporin expression in roots. *Planta* **238**: 669–681
- Paszkowski U, Jakovleva L, Boller T** (2006) Maize mutants affected at distinct stages of the arbuscular mycorrhizal symbiosis. *Plant J* **47**: 165–173
- Plessis A, Hafemeister C, Wilkins O, Gonzaga ZJ, Meyer RS, Pires I, Müller C, Septiningsih EM, Bonneau R, Purugganan MD** (2015) Multiple abiotic stimuli are integrated in the regulation of rice gene expression under field conditions. *eLife* **4**: e08411
- Poorter H, Fiorani F, Pieruschka R, Wojciechowski T, van der Putten WH, Kleyer M, Schurr U Postma J** (2016) Pampered inside, pestered outside? Differences and similarities between plants growing in controlled conditions and in the field. *New Phytol* **212**: 838–855
- Postma M, Goedhart J** (2019) PlotsOfData—a web app for visualizing data together with their summaries. *PLoS Biol* **17**: e3000202

- Prasad KV, Abdel-Hameed AA, Xing D, Reddy AS** (2016) Global gene expression analysis using RNA-seq uncovered a new role for SR1/CAMTA3 transcription factor in salt stress. *Sci Rep* **6**: 27021
- R Core Team (2020) R: A Language and Environment for Statistical Computing. R Foundation for Statistical Computing, Vienna
- Richards CL, Rosas U, Banta JA, Bhambhra N, Purugganan MD** (2012) Genome-wide patterns of Arabidopsis gene expression in nature. *PLoS Genet* **8**: e1002662
- Rosas U, Cibrian-Jaramillo A, Ristova D, Banta JA, Gifford ML, Fan AH, Zhou RW, Kim GJ, Krouk G, Birnbaum KD, et al.** (2013) Integration of responses within and across Arabidopsis natural accessions uncovers loci controlling root systems architecture. *Proc Natl Acad Sci USA* **110**: 15133–15138
- Rosseel Y** (2012) Lavaan: an R package for structural equation modeling. *J Stat Softw* **48**: 1–36
- Sakurai J, Ahamed A, Murai M, Maeshima M, Uemura M** (2008) Tissue and cell-specific localization of rice aquaporins and their water transport activities. *Plant Cell Physiol* **49**: 30–39
- Sakurai J, Ishikawa F, Yamaguchi T, Uemura M, Maeshima M** (2005) Identification of 33 rice aquaporin genes and analysis of their expression and function. *Plant Cell Physiol* **46**: 1568–1577
- Sandhu N, Raman KA, Torres RO, Audebert A, Dardou A, Kumar A, Henry A** (2016) Rice root architectural plasticity traits and genetic regions for adaptability to variable cultivation and stress conditions. *Plant Physiol* **171**: 2562–2576
- Santosh Kumar, VV, Yadav SK, Verma RK, Shrivastava S, Ghimire O, Pushkar S, Rao MV, Senthil Kumar T, Chinnusamy V** (2021) The abscisic acid receptor OsPYL6 confers drought tolerance to indica rice through dehydration avoidance and tolerance mechanisms. *J Exp Bot* **72**: 1411–1431
- Shrestha R, Gómez-Ariza J, Brambilla V, Fornara F** (2014) Molecular control of seasonal flowering in rice, Arabidopsis and temperate cereals. *Ann Bot* **114**: 1445–1458
- Singh A, Singh Y, Mahato AK, Jayaswal PK, Singh S, Singh R, Yadav N, Singh AK, Singh PK, Singh R, et al.** (2020) Allelic sequence variation in the *Sub1A*, *Sub1B* and *Sub1C* genes among diverse rice cultivars and its association with submergence tolerance. *Sci Rep* **10**: 8621
- Storey JD, Tibshirani R** (2003) Statistical significance for genome-wide studies. *Proc Natl Acad Sci USA* **100**: 9440–9445
- Swift J, Adame M, Tranchina D, Henry A, Coruzzi GM** (2019) Water impacts nutrient dose responses genome-wide to affect crop production. *Nat Commun* **10**: 1374
- Tang N, Shahzad Z, Lonjon F, Loudet O, Vaillau F, Maurel C** (2018) Natural variation at XND1 impacts root hydraulics and trade-off for stress responses in Arabidopsis. *Nat Commun* **9**: 3884
- Todaka D, Shinozaki K, Yamaguchi-Shinozaki, K** (2015) Recent advances in the dissection of drought-stress regulatory networks and strategies for development of drought-tolerant transgenic rice plants. *Front Plant Sci* **6**: 84
- Tardieu F, Simonneau T** (1998) Variability among species of stomatal control under fluctuating soil water status and evaporative demand: modelling isohydric and anisohydric behaviours. *J Exp Bot* **49**: 419–432
- Torres RO, McNally KL, Cruz CV, Serraj R, Henry A** (2013) Screening of rice Genebank germplasm for yield and selection of new drought tolerance donors. *Field Crops Res* **147**: 12–22
- Turner NC** (2018) Turgor maintenance by osmotic adjustment: 40 years of progress. *J Exp Bot* **69**: 3223–3233
- Uga Y, Sugimoto K, Ogawa S, Rane J, Ishitani M, Hara N, Kitomi Y, Inukai Y, Ono K, Kanno N, et al.** (2013) Control of root system architecture by DEEPER ROOTING 1 increases rice yield under drought conditions. *Nat Genet* **45**: 1097–1102
- Valladares F, Sanchez-Gomez D, Zavala MA** (2006) Quantitative estimation of phenotypic plasticity: bridging the gap between the evolutionary concept and its ecological applications. *J Ecol* **94**: 1103–1116
- de Vries FT, Griffiths RI, Knight CG, Nicolitch O, Williams A** (2020) Harnessing rhizosphere microbiomes for drought-resilient crop production. *Science* **368**: 270–274
- Wang F, Coe RA, Karki S, Wanchana S, Thakur V, Henry A, Lin HC, Huang J, Peng S, Quick WP** (2016) Overexpression of OsSAP16 regulates photosynthesis and the expression of a broad range of stress response genes in rice (*Oryza sativa* L.). *PLoS ONE* **11**: e0157244
- Wang W, Mauleon R, Hu Z, Chebotarov D, Tai S, Wu Z, Li M, Zheng T, Fuentes RR, Zhang F, et al.** (2018) Genomic variation in 3,010 diverse accessions of Asian cultivated rice. *Nature* **557**: 43–49
- Wang Y, Wan L, Zhang L, Zhang Z, Zhang H, Quan R, Zhou S, Huang R** (2012) An ethylene response factor OsWR1 responsive to drought stress transcriptionally activates wax synthesis related genes and increases wax production in rice. *Plant Mol Biol* **78**: 275–288
- Welch BL** (1947) The generalisation of Student's problems when several different population variances are involved. *Biometrika* **34**: 28–35
- Wilkins O, Hafemeister C, Plessis A, Holloway-Phillips MM, Pham GM, Nicotra AB, Gregorio GB, Jagadish SK, Septiningsih EM, Bonneau R, et al.** (2016) EGRINs (Environmental Gene Regulatory Influence Networks) in rice that function in the response to water deficit, high temperature, and agricultural environments. *Plant Cell* **28**: 2365–2384
- Wing RA, Purugganan MD, Zhang Q** (2018) The rice genome revolution: from an ancient grain to Green Super Rice. *Nat Rev Genet* **19**: 505–517
- Wolak ME, Fairbairn DJ, Paulsen YR** (2012) Guidelines for estimating repeatability. *Methods Ecol Evol* **3**: 129–137
- Xu K, Xu X, Fukao T, Canlas P, Maghirang-Rodriguez R, Heuer S, Ismail AM, Bailey-Serres J, Ronald PC, Mackill DJ** (2006) Sub1A is an ethylene-response-factor-like gene that confers submergence tolerance to rice. *Nature* **442**: 705–708
- Yang A, Dai X, Zhang WH** (2012b) A R2R3-type MYB gene, OsMYB2, is involved in salt, cold, and dehydration tolerance in rice. *J Exp Bot* **63**: 2541–2556
- Yang SY, Grønlund M, Jakobsen I, Grottemeyer MS, Rentsch D, Miyao A, Hirochika H, Kumar CS, Sundaresan V, Salamin N, et al.** (2012a) Nonredundant regulation of rice arbuscular mycorrhizal symbiosis by two members of the PHOSPHATE TRANSPORTER1 gene family. *Plant Cell* **24**: 4236–4251
- Yao X, Ma H, Wang J, Zhang D** (2007) Genome-wide comparative analysis and expression pattern of TCP gene families in *Arabidopsis thaliana* and *Oryza sativa*. *J Integr Plant Biol* **49**: 885–897
- Yu P, Wang C, Baldauf JA, Tai H, Gutjahr C, Hochholdinger F, Li C** (2018) Root type and soil phosphate determine the taxonomic landscape of colonizing fungi and the transcriptome of field-grown maize roots. *New Phytol* **217**: 1240–1253
- Zaidem ML, Groen SC, Purugganan MD** (2019) Evolutionary and ecological functional genomics, from lab to the wild. *Plant J* **97**: 40–55
- Zhang C, Li C, Liu J, Lv Y, Yu C, Li H, Zhao T, Liu B** (2017) The OsABF1 transcription factor improves drought tolerance by activating the transcription of *COR413-TM1* in rice. *J Exp Bot* **68**: 4695–4707.
- Zou M, Guan Y, Ren H, Zhang F, Chen F** (2008) A bZIP transcription factor, OsAB15, is involved in rice fertility and stress tolerance. *Plant Mol Biol* **66**: 675–683